

Hydrogen Embrittlement Fundamentals, Modeling, and Experiment

P. Sofronis, I. M. Robertson, D. D. Johnson
University of Illinois at Urbana-Champaign

In collaboration with

B. Somerday
Sandia National Laboratories



DOE Hydrogen Pipeline Working Group Meeting
September 25, 2007

Hydrogen Embrittlement Mechanisms

- **Several candidate mechanisms have evolved over the years each of which is supported by a set of experimental observations and strong personal views**

- **Viable mechanisms of embrittlement**
 - **Stress induced hydride formation and cleavage**
 - Metals with stable hydrides (Group Vb metals, Ti, Mg, Zr and their alloys)
 - Supported by experimental observations
 - **Hydrogen enhanced localized plasticity (HELP)**
 - Increased dislocation mobility, failure by plastic deformation mechanisms
 - Supported by experimental observations
 - **Hydrogen induced decohesion**
 - Direct evidence is lacking
 - Supported by First Principles Calculations (DFT)

- **Degradation is often due to the synergistic action of mechanisms**

Embrittlement and Phenomenology

- **Fractographic evidence suggests that low strength steels under static loading fail by**
 - Hydrogen-assisted **transgranular fracture** induced by void or microcrack initiation through decohesion at internal interface (precipitate/inclusion or phase boundaries) ahead of a crack or notch accompanied by shear localization (HELP) leading to the linking of the void/microcrack with the tip of the crack
 - Fracture is controlled by yield strength level and microstructure

- **Our contention, which needs to be verified through experiment, is that embrittlement**
 - **Under static load** is a result of the synergistic action of the HELP and decohesion mechanisms
 - **Under cyclic load** can be intergranular (extremely dangerous mode of failure)

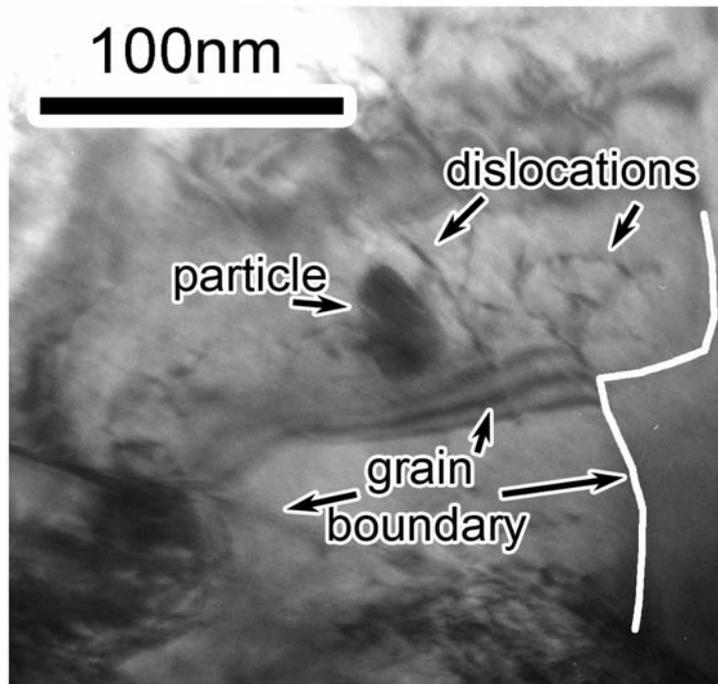
New Steel Microstructure-Oregon Steel Mills (OSM)

4

API Grade	C	Mn	Si	Cu	Ni	V	Nb	Cr	Ti
X70/80	0.04	1.61	0.14	0.22	0.12	0.000	0.096	0.42	0.015

acicular ferrite microstructure

Defects in microstructure, particularly precipitates, act as trap sites for hydrogen

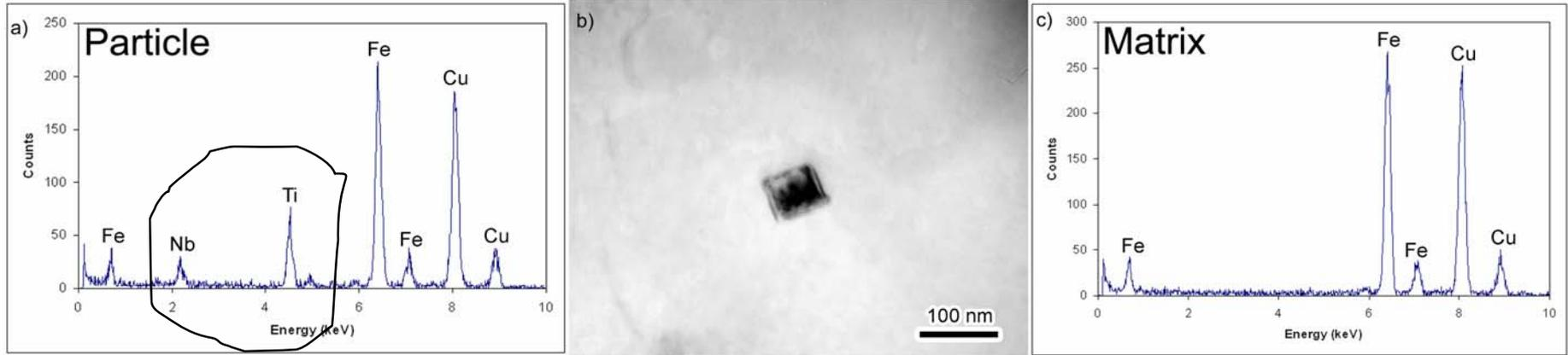


- High dislocation density in some regions
- Irregular grain boundaries and small grains, indicative of microstructure that has not been fully recrystallized and recovered.

Relatively low precipitate density (inside the matrix)

Particle Composition

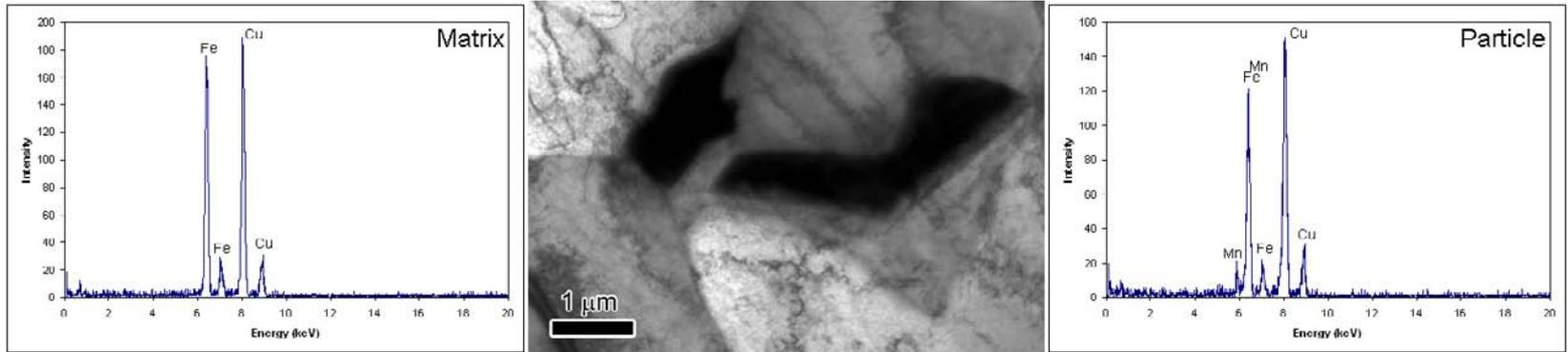
Energy Dispersive Spectroscopy



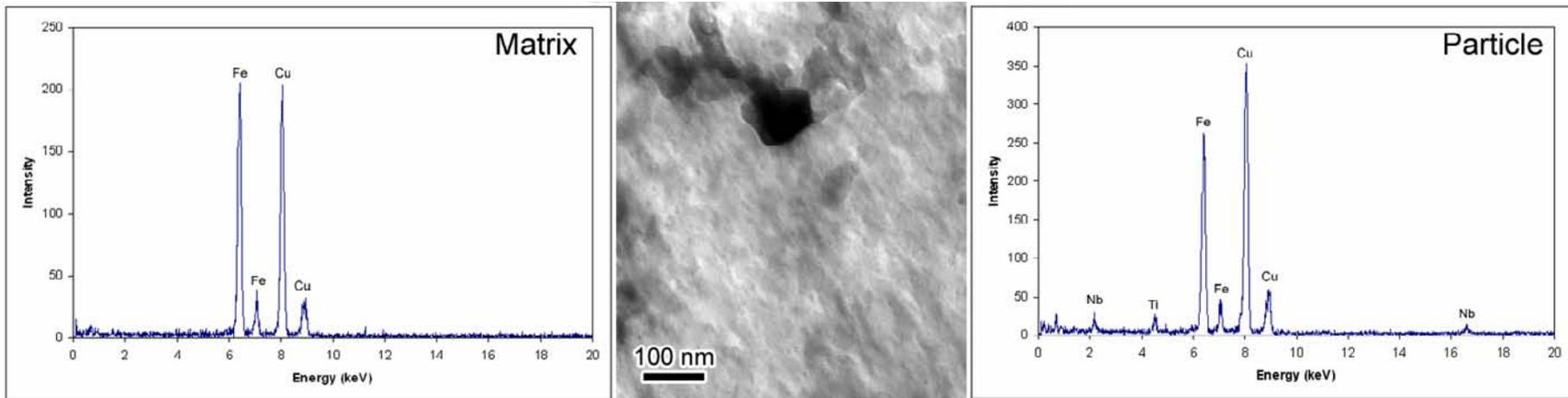
- a) EDS spectrum from particle
- b) Bright field TEM image of typical rectangular particle
- c) EDS spectrum from matrix
- EDS analysis of fine precipitate inside ferrite grain suggests that precipitate is composed of Ti and Nb

(window detector: C, N, O not detected)

Steel Microstructure-Air Liquide Pipeline

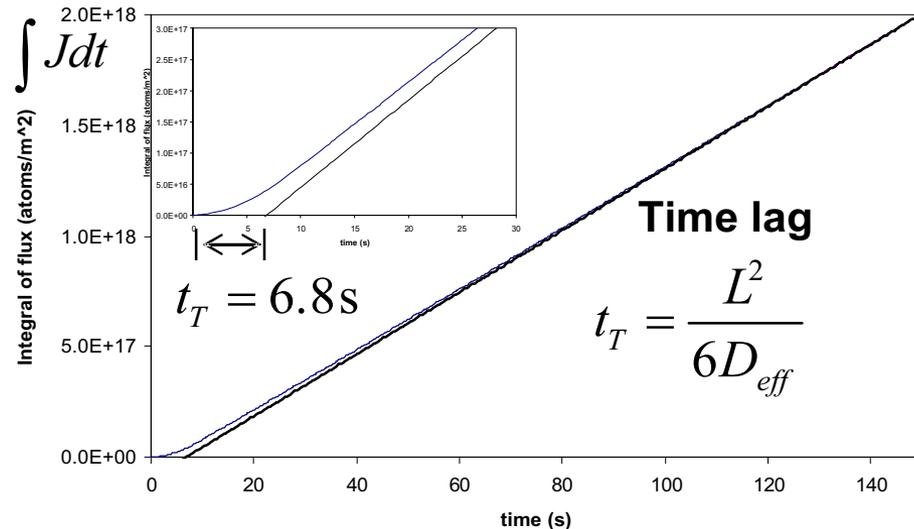
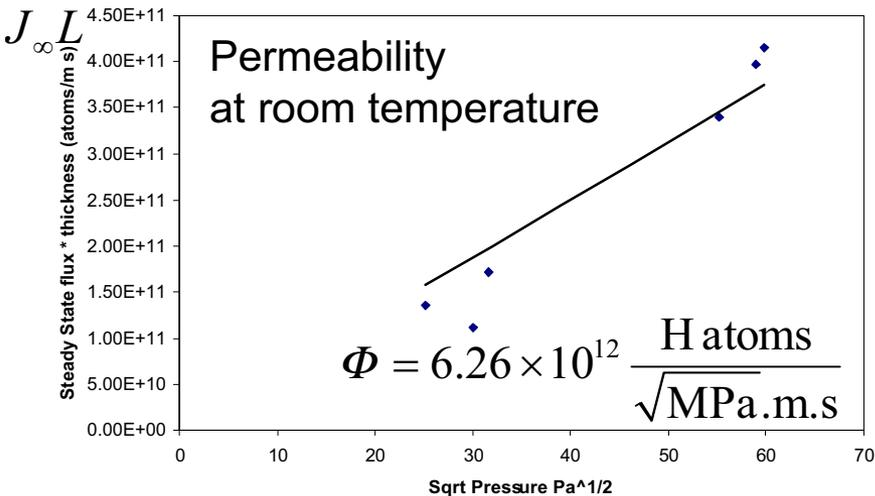
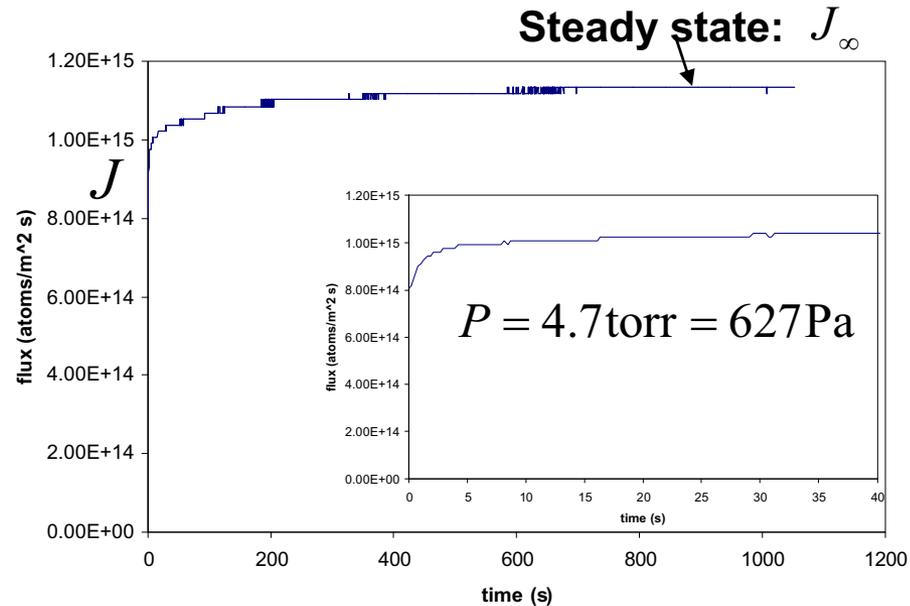
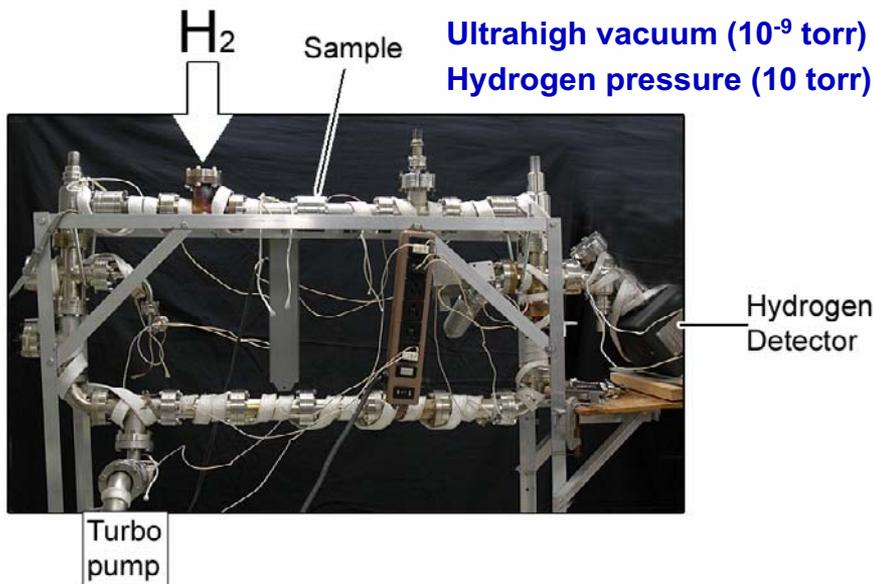


Large intergranular particles (cementite)



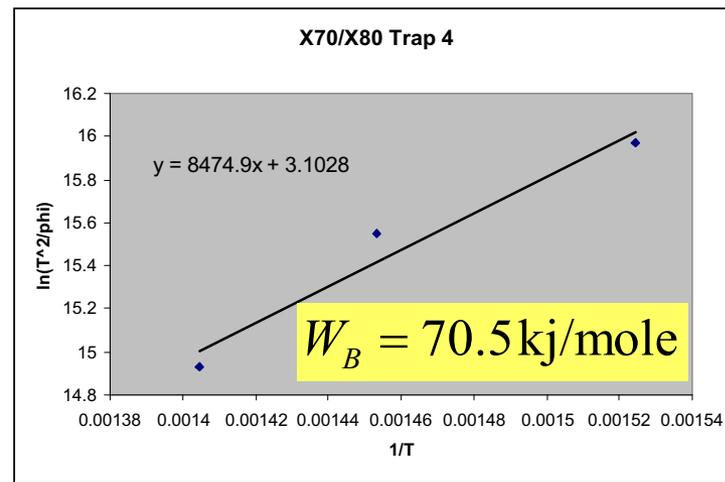
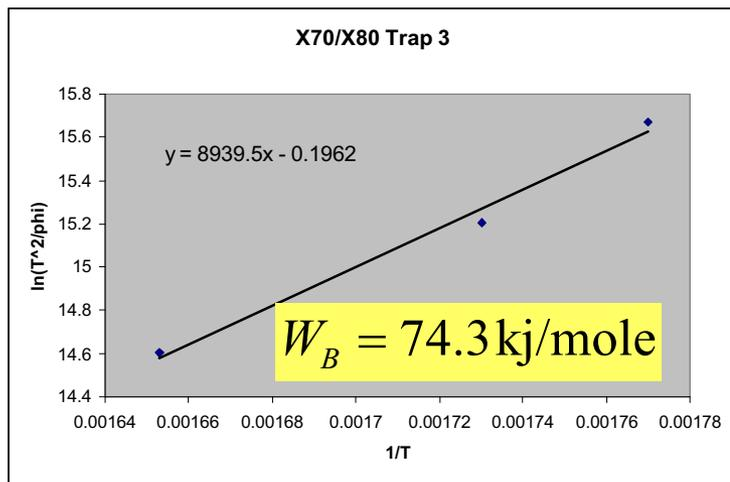
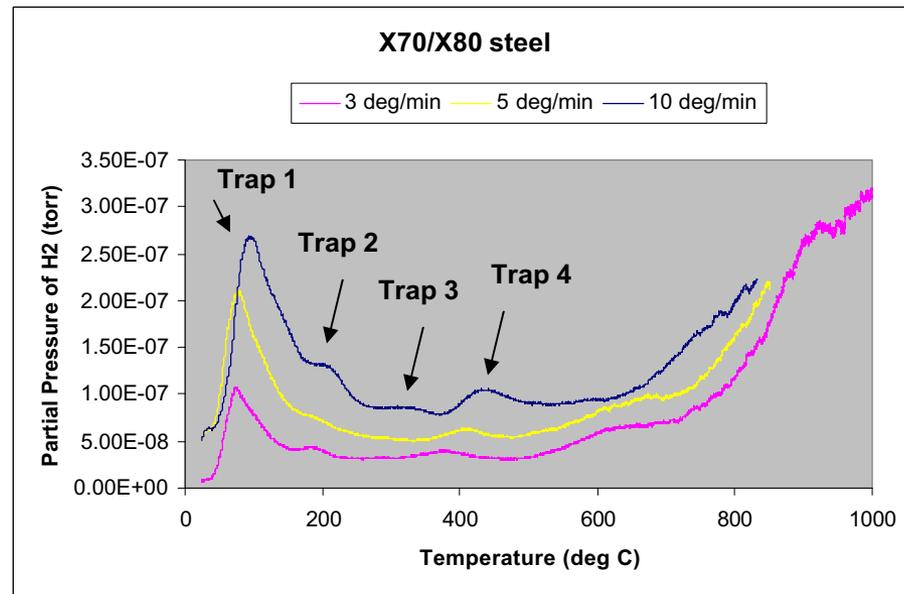
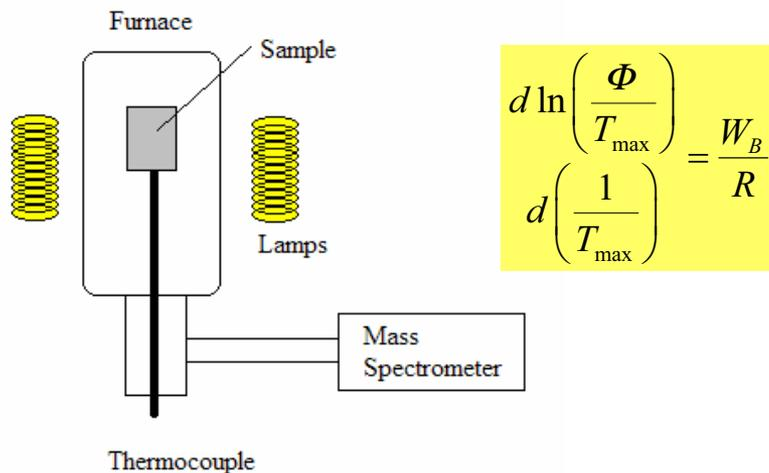
Small intragranular particles (carbides with Nb and Ti)

Hydrogen Permeation Measurements



- Oregon Steel Mills sample: thickness $L = 120$ microns
- room temperature

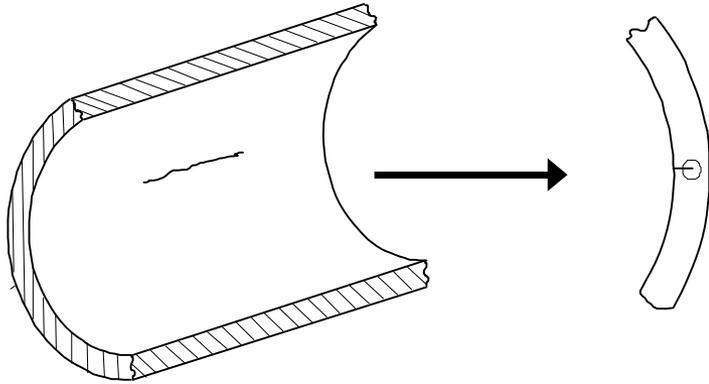
Thermal Desorption Spectroscopy



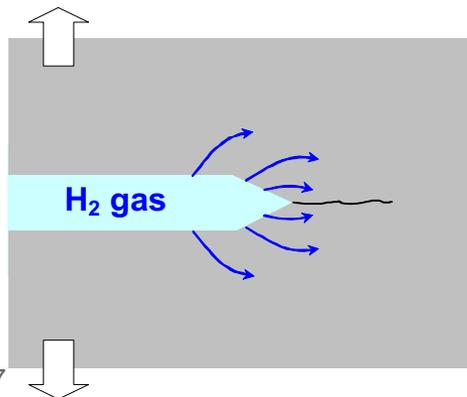
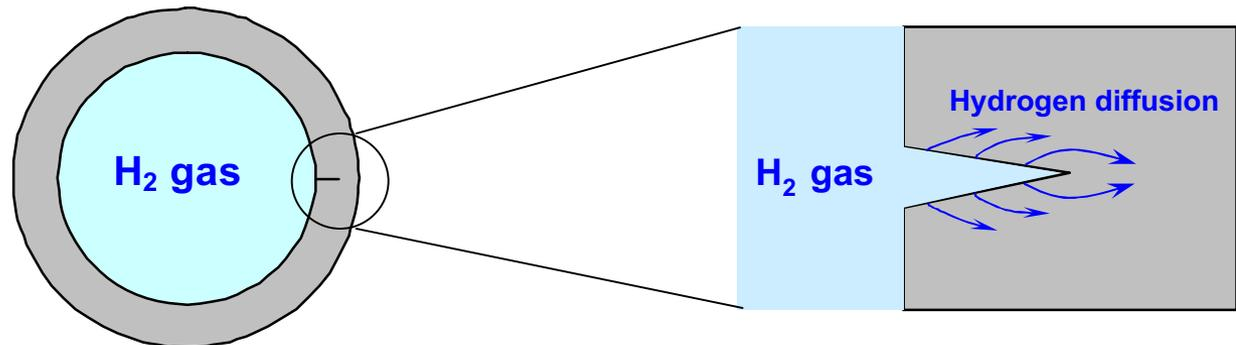
Materials Characterization

- **TEM and TDS**
 - will provide the trap binding energy.
- **Permeation studies along with numerical simulation of diffusion transients**
 - Will validate the trap binding energy determination
 - Will provide the trap density
- **Coated samples (SECAT)**
- **Similar coordinated approach is needed to identify the fracture mechanisms under all loading scenarios**
 - Rising load fracture toughness
 - Subcritical crack growth
 - Fatigue

Fracture Mechanics Approach to Design



Determine the stress, deformation, and hydrogen concentration fields ahead of an axial crack in a pipeline

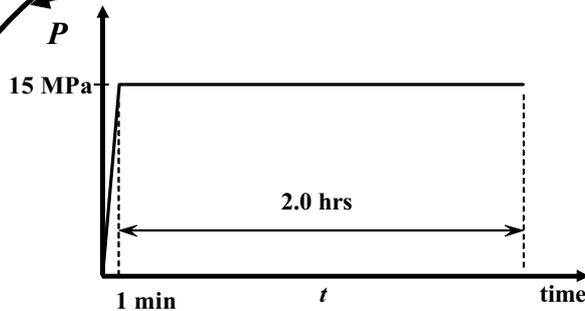


Case study related to subcritical crack growth experiments carried out at Sandia

Cracked Pipeline: Problem Statement

$$C_L(t) = 0$$

$$C_L(t) = K \times \sqrt{f}$$



Hydrogen gas
at pressure P

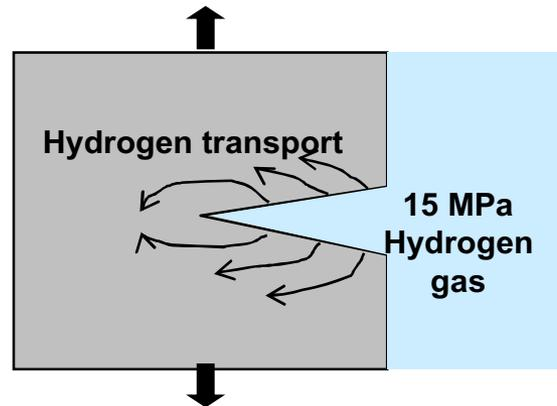
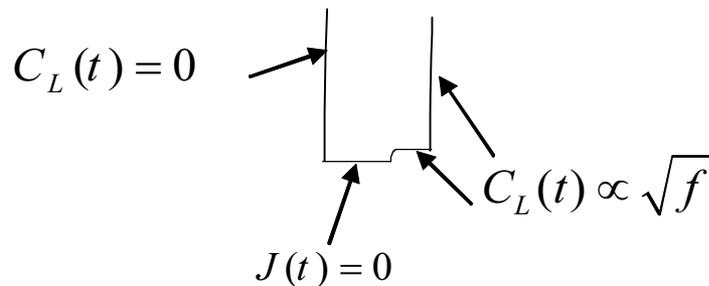
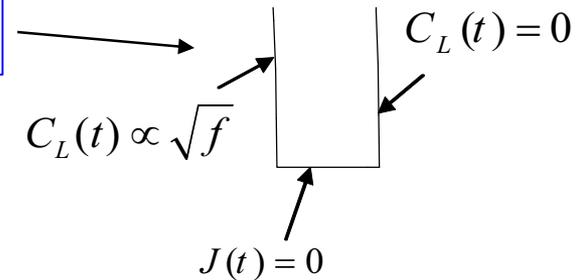
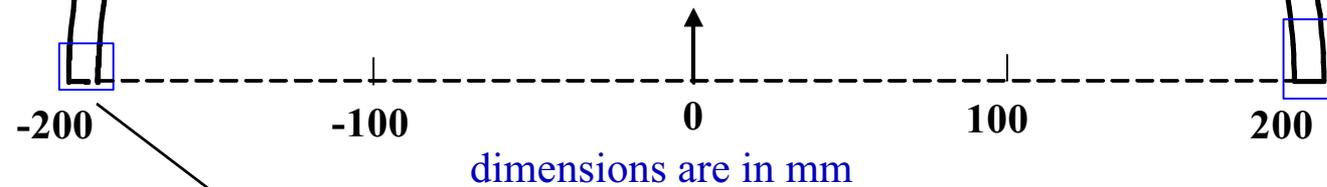
outer diameter: 40.64 cm

thickness: $h = 9.52$ mm

crack depth: $a = 1.9$ mm

initial CTOD: $b_0 = 1.5$ μm

$a/h = 0.2$



K : Solubility

J : Hydrogen flux

P : Pressure

f : Fugacity

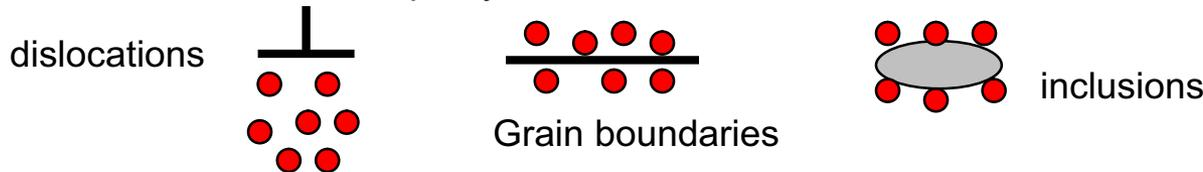
Hydrogen Transport Analysis

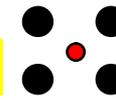
■ Diffusing hydrogen resides at

- Normal Interstitial Lattice Sites (NILS) $C_L = \beta \theta_L N_L$

- Trapping Sites $C_T = \alpha \theta_T N_T$

- Microstructural heterogeneities such as dislocations, grain boundaries, inclusions, voids, interfaces, impurity atom clusters





 θ_L = NILS occupancy
 β = number of NILS per solvent atom.
 N_L = number of solvent atoms/m³.

θ_T = trap occupancy
 α = number of sites per trap.
 N_T = number of traps/m³.

■ Hydrogen populations in NILS and trapping sites are assumed to be in equilibrium according to Oriani's theory

$$\frac{\theta_T}{1-\theta_T} = \frac{\theta_L}{1-\theta_L} \exp\left(\frac{W_B}{RT}\right)$$

W_B = Trap binding energy

T=Temperature

R=gas constant

- Trap density may evolve dynamically with plastic straining

■ Hydrogen Transport Equation

$$\frac{D}{D_{eff}} \frac{dC_L}{dt} = DC_{L,ii} - \left(\frac{DV_H}{3RT} C_L \sigma_{kk,i} \right)_{,i} - \alpha \theta_T \frac{\partial N_T}{\partial \epsilon^p} \frac{d\epsilon^p}{dt}$$

- Note the effect of stress and plastic strain

d/dt = time differentiation

C = Hydrogen concentration

D = diffusion coefficient

D_{eff} = Effective diffusion

$= D / (1 + \partial C_T / \partial C_L)$ accounting for trapping

σ_{kk} = hydrostatic stress

ϵ^p = plastic strain

V_H = partial molar volume of H

N_T = trap density

$()_{,i} = \partial() / \partial x_i$

Material: X70/80 acicular ferrite microstructure

$$C = K\sqrt{f} \quad f = P \exp\left(\frac{Pd}{RT}\right) \quad d = 15.84 \text{ cm}^3/\text{mol}$$

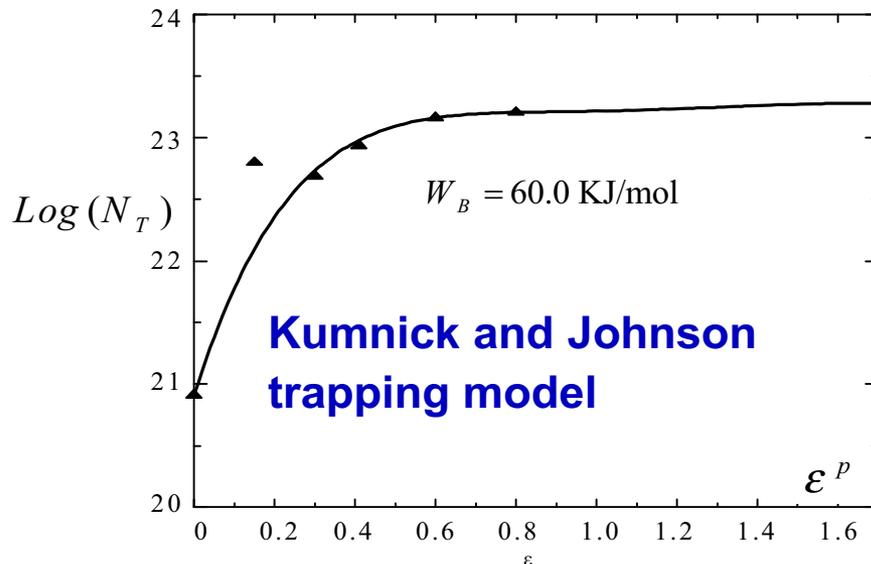
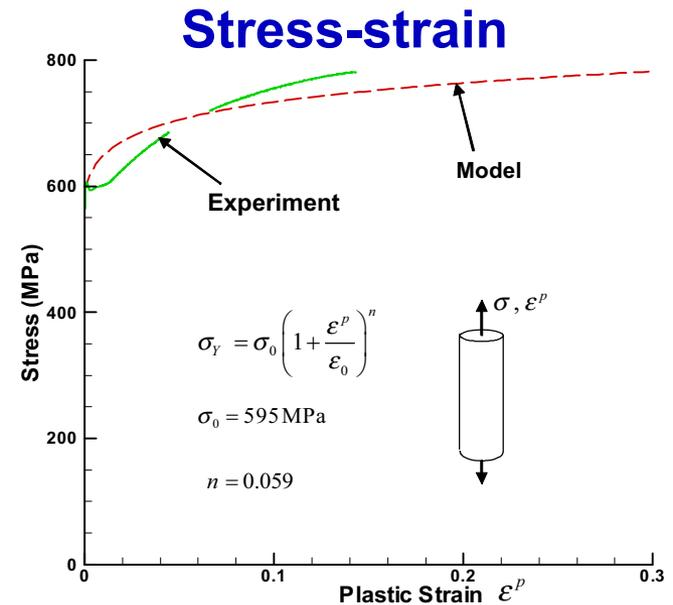
$$K = 6.54696 \times 10^{18} \frac{\text{H atoms}}{\text{m}^3 \sqrt{\text{Pa}}}$$

$$C_0 = 2.084 \times 10^{21} \text{ H atom} / \text{m}^3 \quad P = 1 \text{ atm}$$

$$C_0 = 2.65932 \times 10^{22} \text{ H atom} / \text{m}^3 \quad P = 15 \text{ MPa}$$

Lattice diffusion coefficient

$$D = 1.271 \times 10^{-8} \text{ m}^2/\text{s}$$



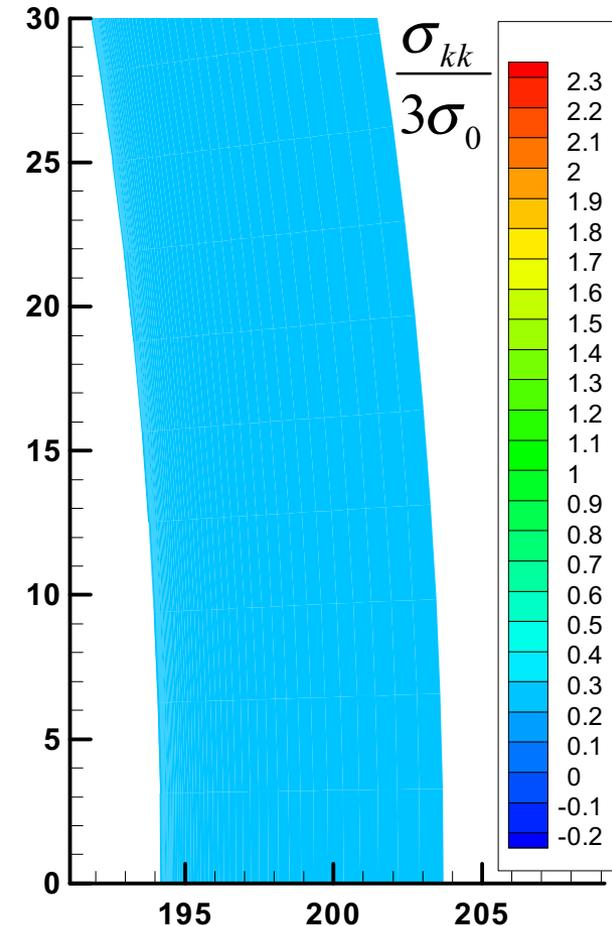
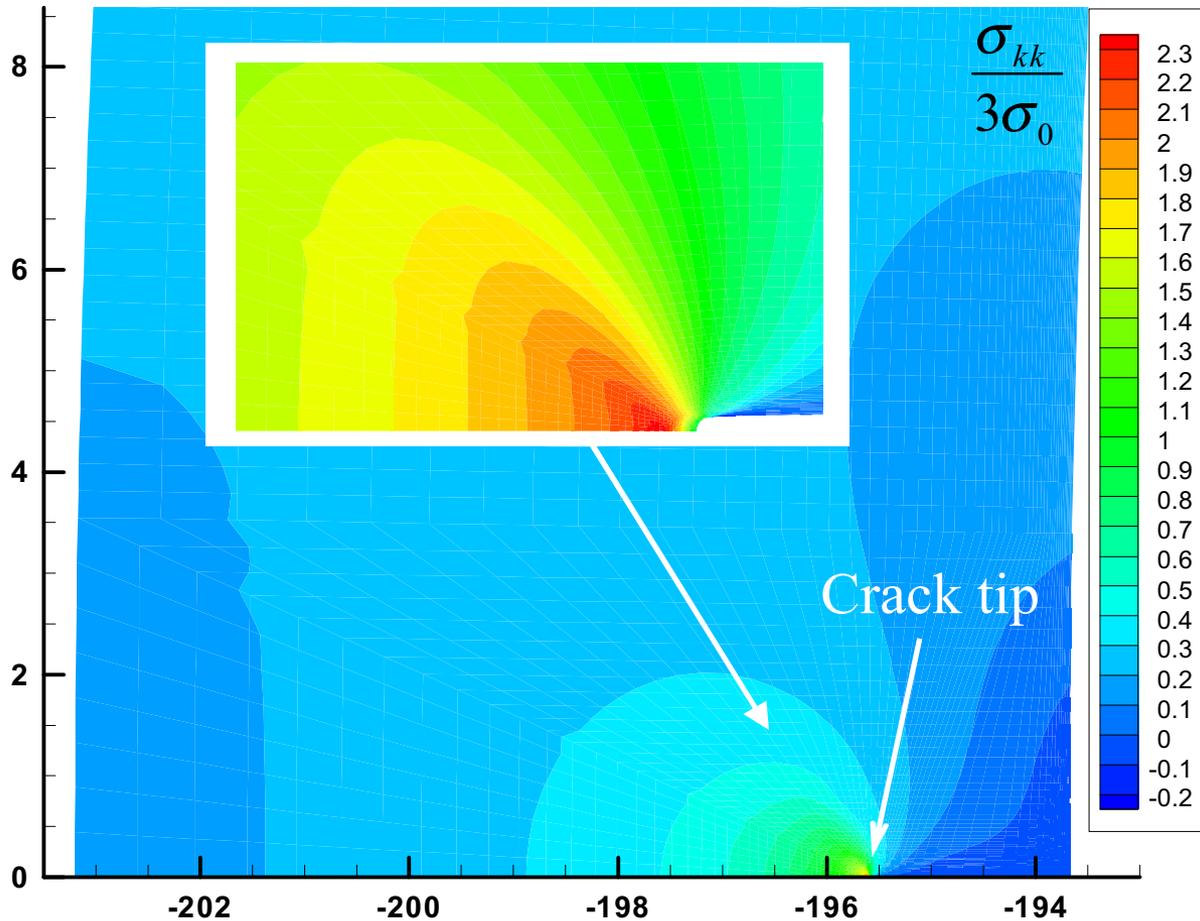
Dislocation trapping modeling

$$N_T = \frac{\sqrt{2}\rho}{a} \quad W_B = 20.2 \text{ KJ/mol}$$

$$\rho = \begin{cases} \rho_0 + \frac{\gamma}{0.15} \epsilon^p & \epsilon^p \leq 0.15 \\ \text{const.} & \epsilon^p > 0.15 \end{cases}$$

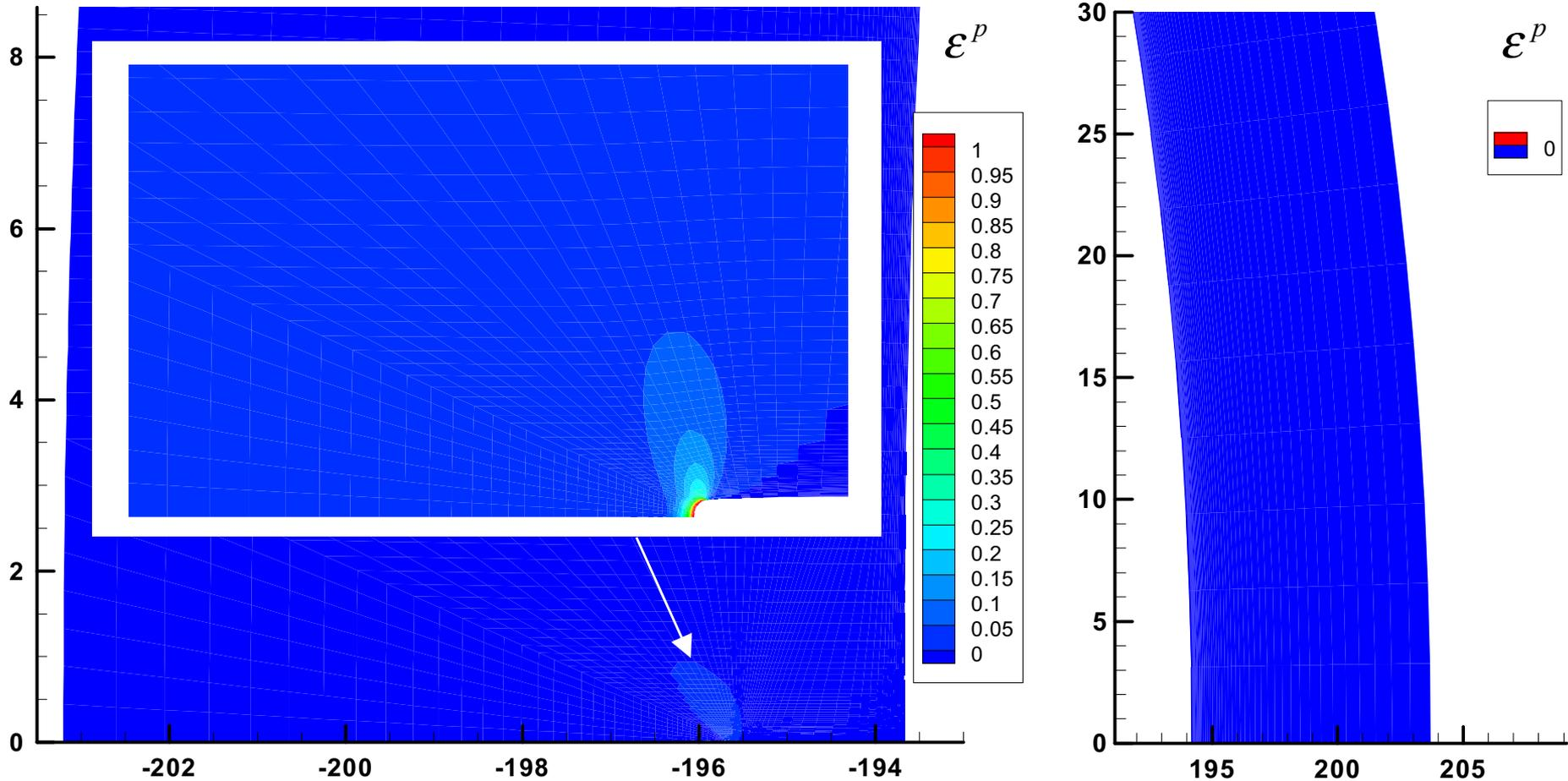
$$\rho_0 = 10^{10} \text{ m}^{-2}, \quad \gamma = 10^{16} \text{ m}^{-2}$$

Hydrostatic Stress at Pressure 15 MPa



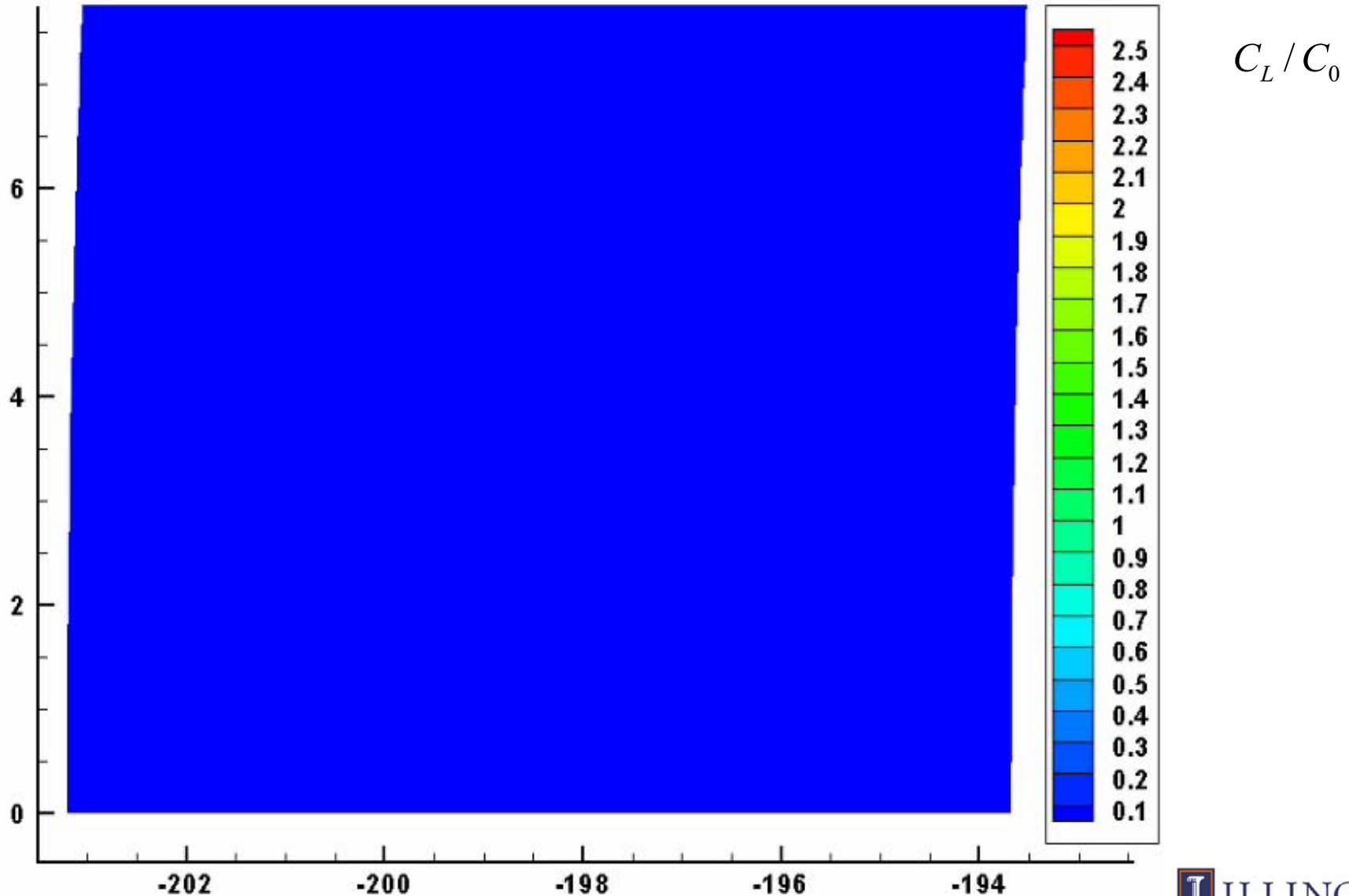
Geometric dimensions are in mm

Plastic Strain at Pressure 15 MPa



Geometric dimensions are in mm

Lattice Concentration Toward Steady State

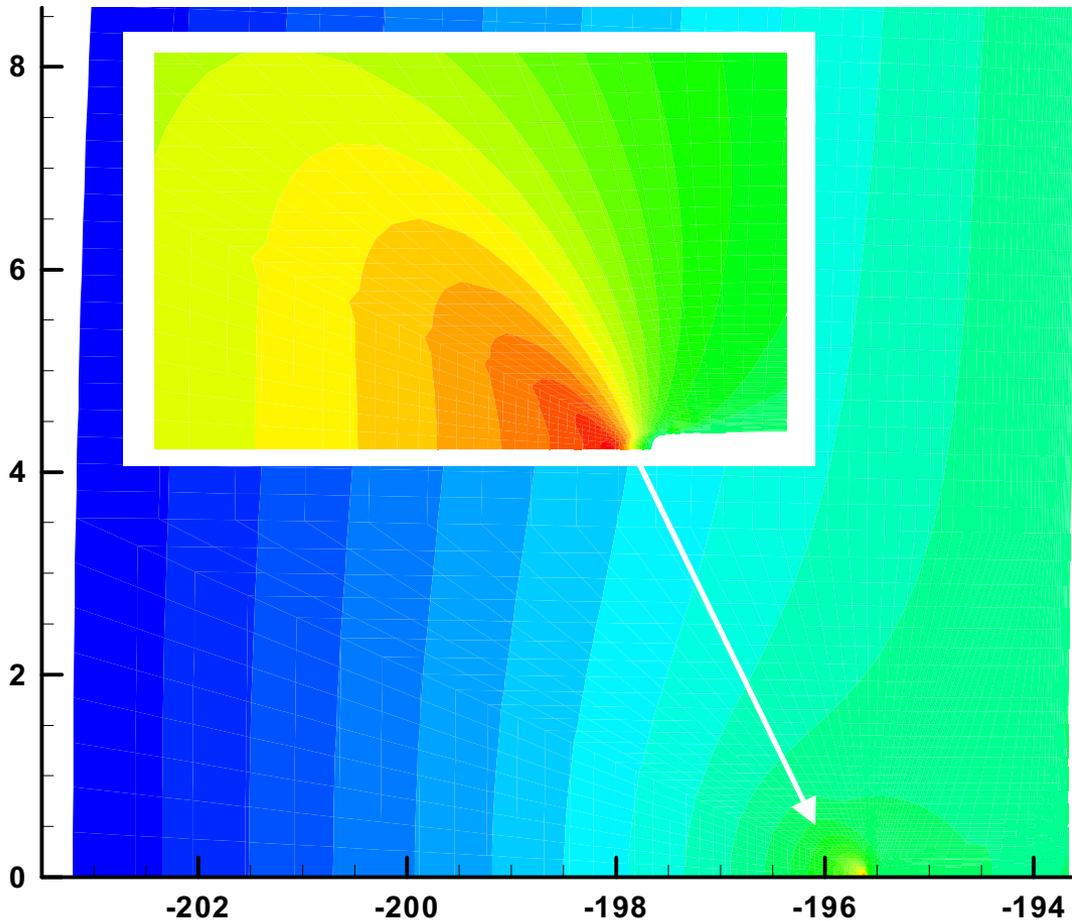


Lattice Hydrogen Concentration at Steady State

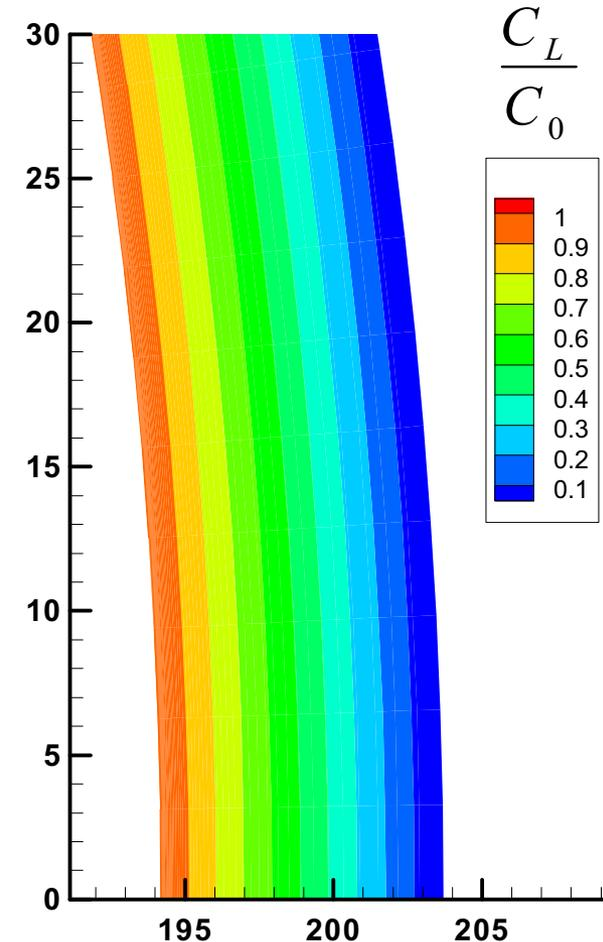
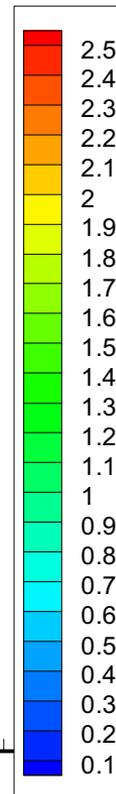
Kumnick and Johnson trapping model

Time to steady-state: 2.0 hrs

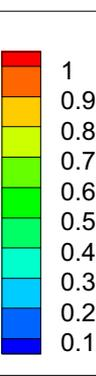
$t_{ss} = 8 \text{ min } 40 \text{ sec}$



$\frac{C_L}{C_0}$



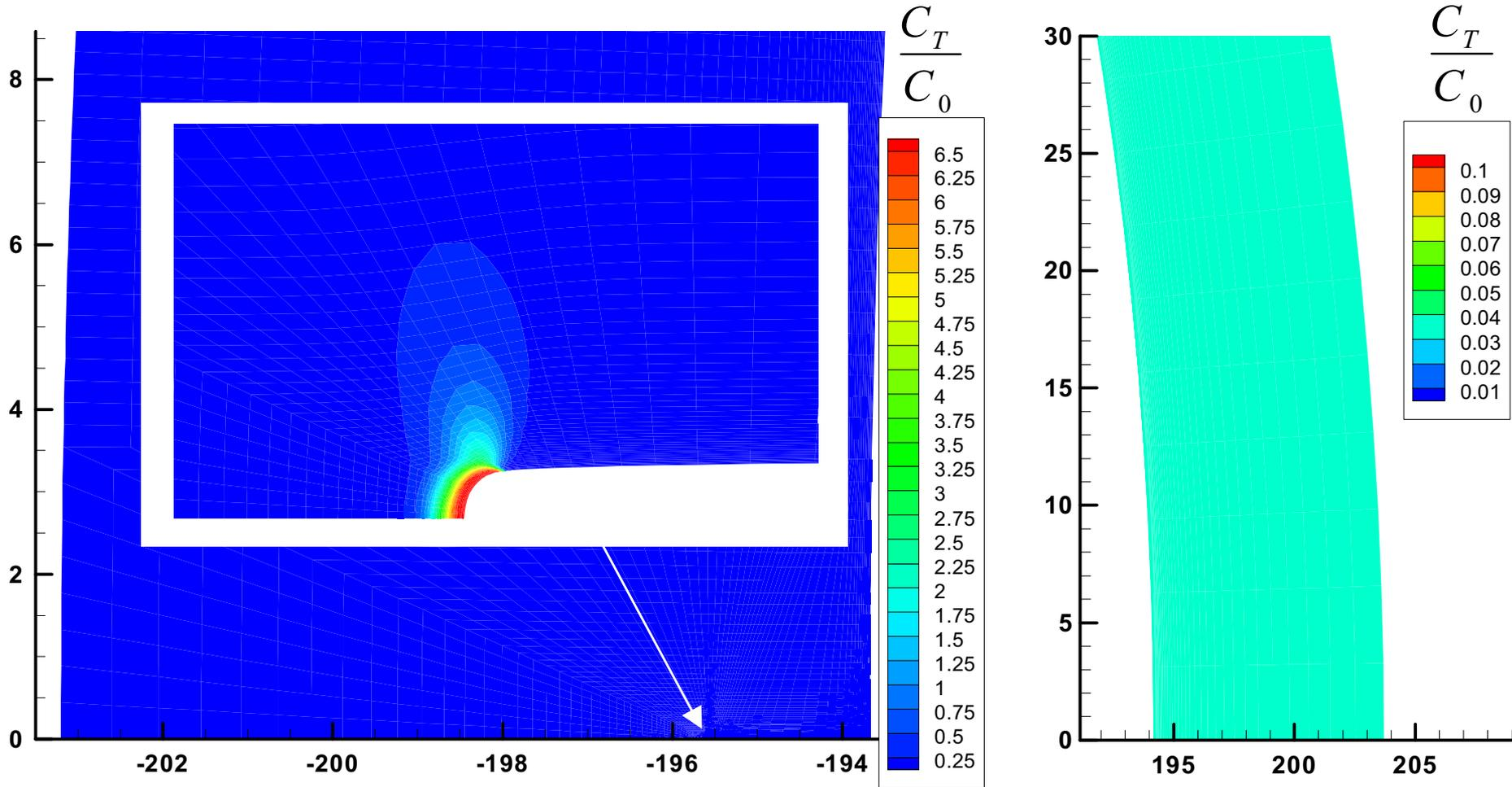
$\frac{C_L}{C_0}$



$$C_0 = 2.65932 \times 10^{22} \text{ H atom / m}^3 \quad P = 15 \text{ MPa}$$

Trapped Hydrogen Concentration at Steady State

Kumnick and Johnson trapping model



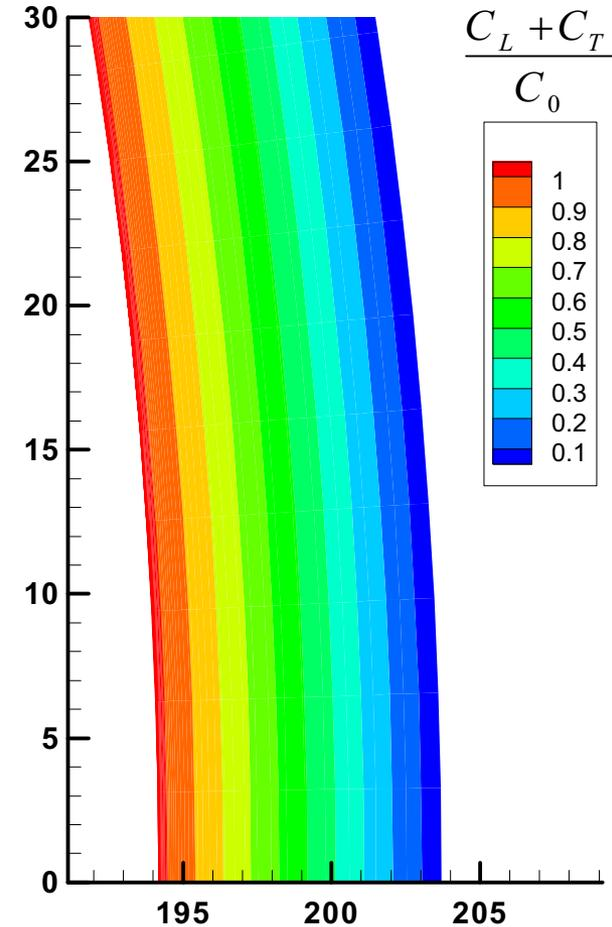
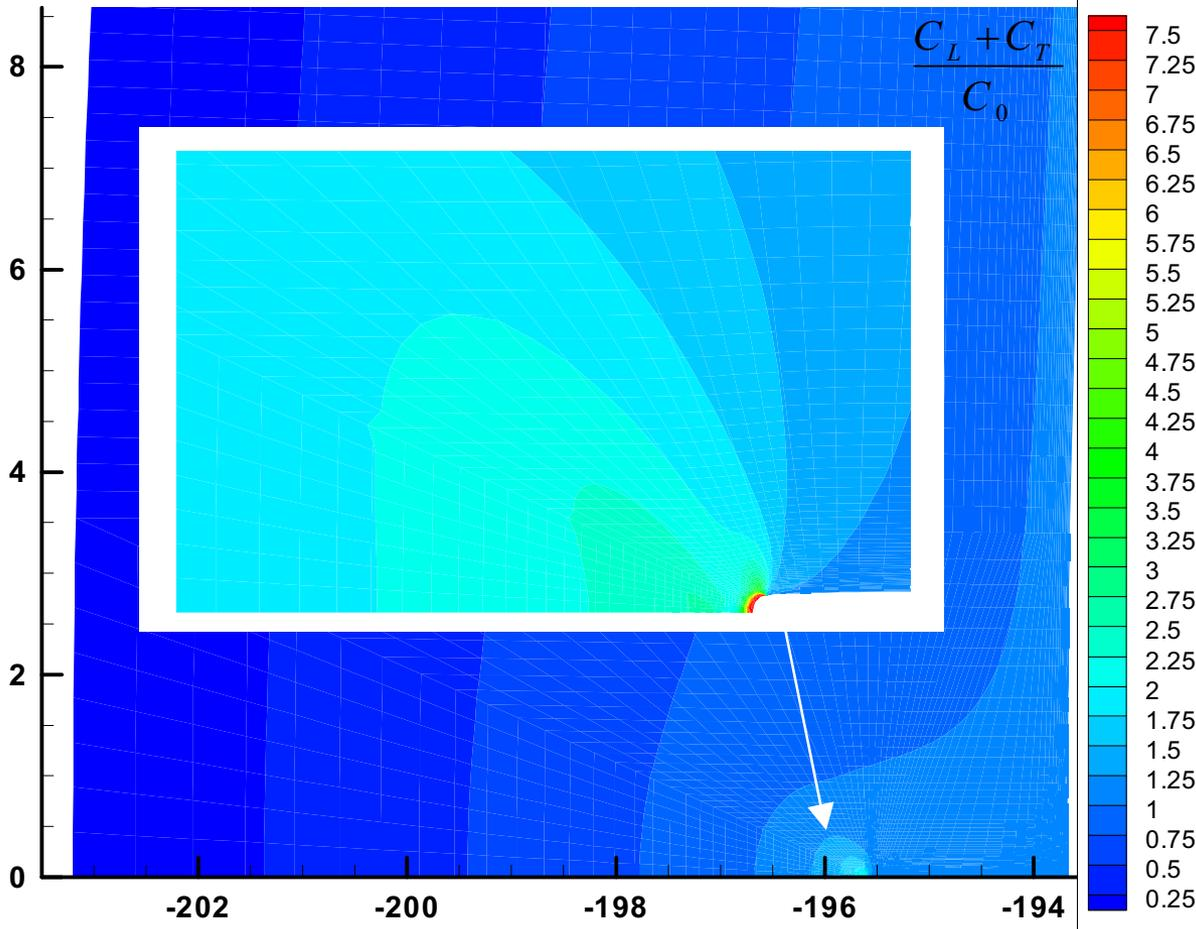
$$C_0 = 2.65932 \times 10^{22} \text{ H atom / m}^3 \quad P = 15 \text{ MPa}$$

Total Hydrogen Concentration at Steady State

Kumnick and Johnson
trapping model

Time to steady-state is 2.0 hrs

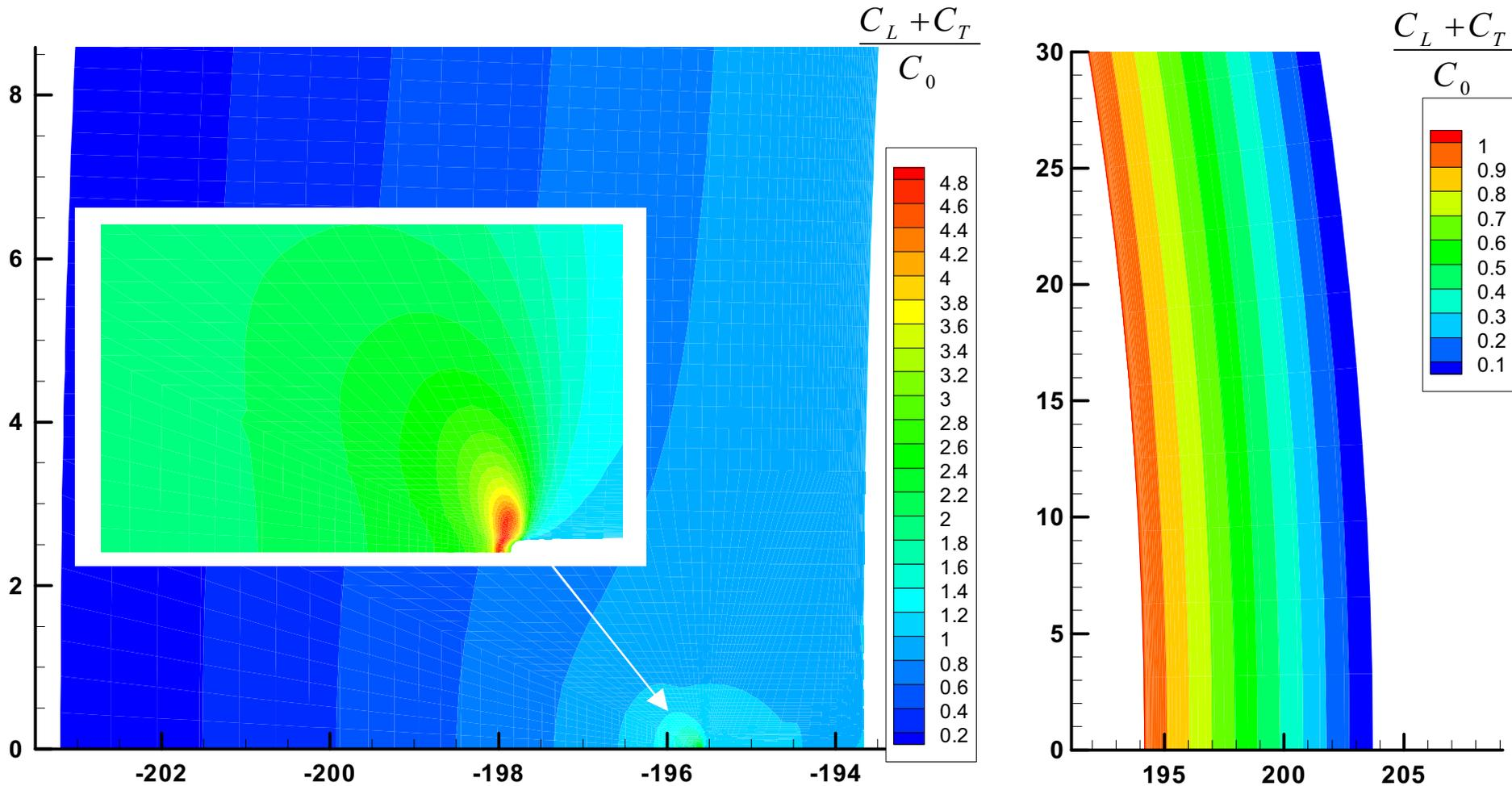
$$t_{ss} = 8 \text{ min } 40 \text{ sec}$$



$$C_0 = 2.65932 \times 10^{22} \text{ H atom / m}^3 \quad P = 15 \text{ MPa}$$

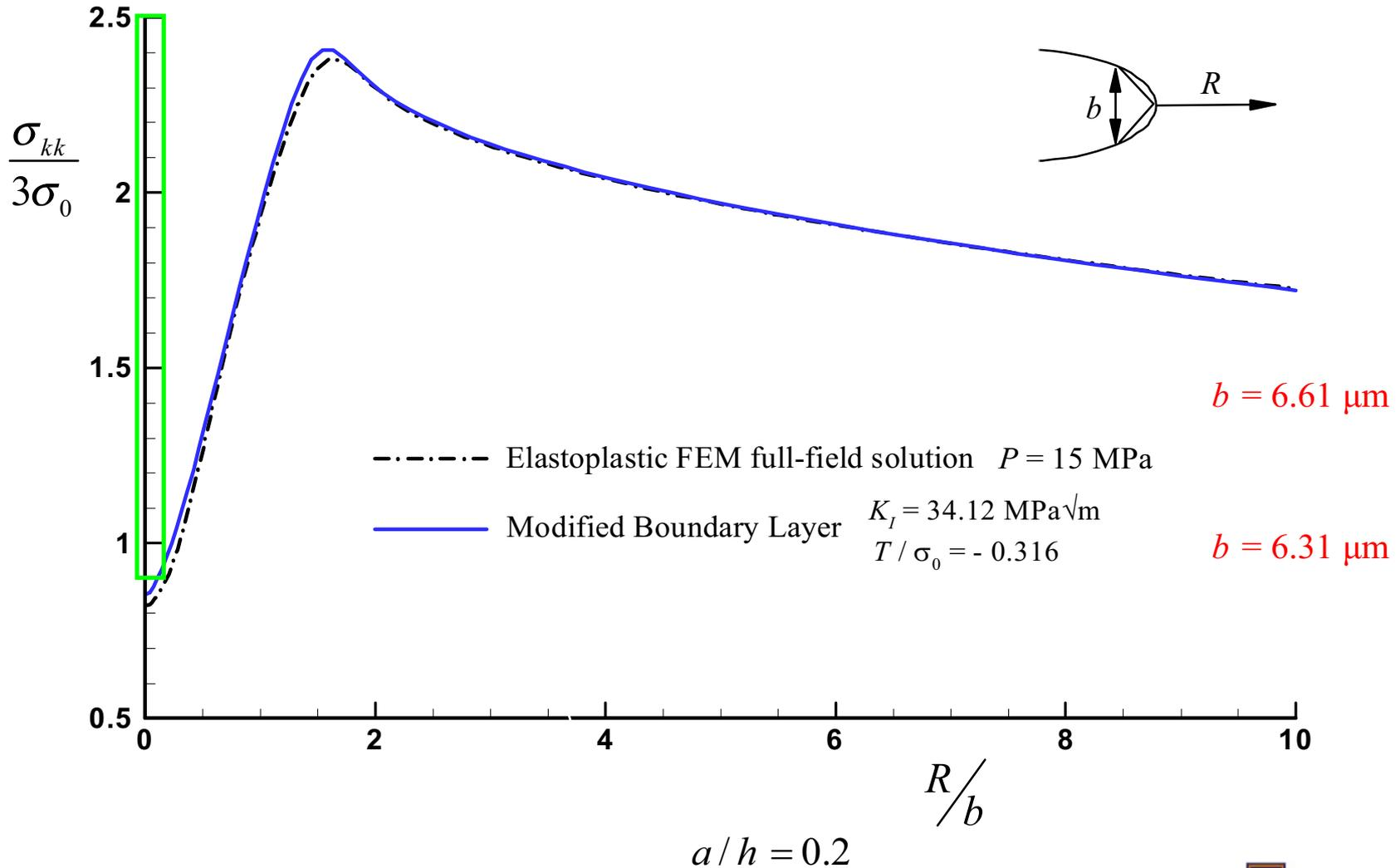
Total Hydrogen Concentration at Steady State

Dislocation trapping model



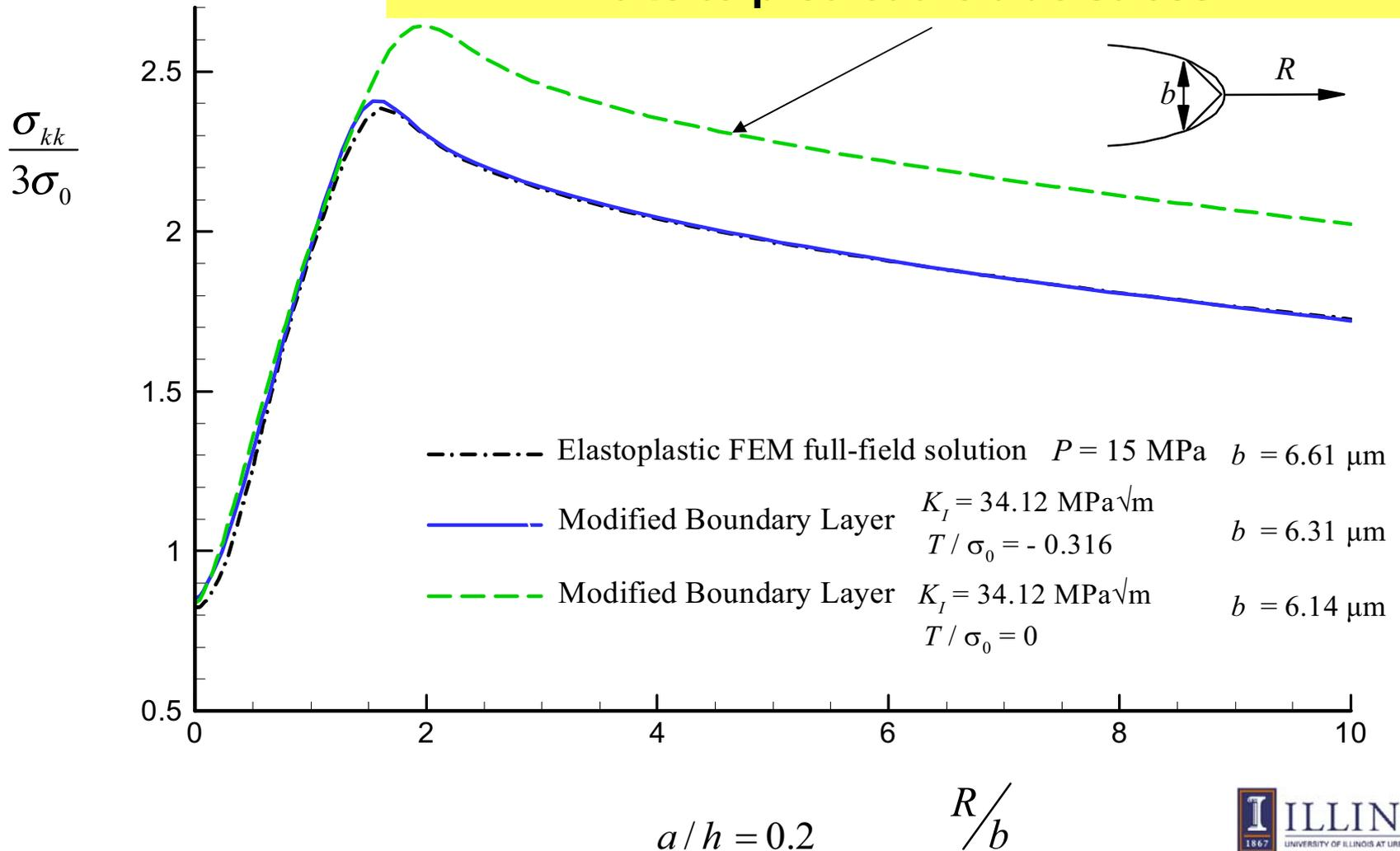
$$C_0 = 2.65932 \times 10^{22} \text{ H atom / m}^3 \quad P = 15 \text{ MPa}$$

Full Field (pipeline) vs Boundary Layer Solution (laboratory specimen)

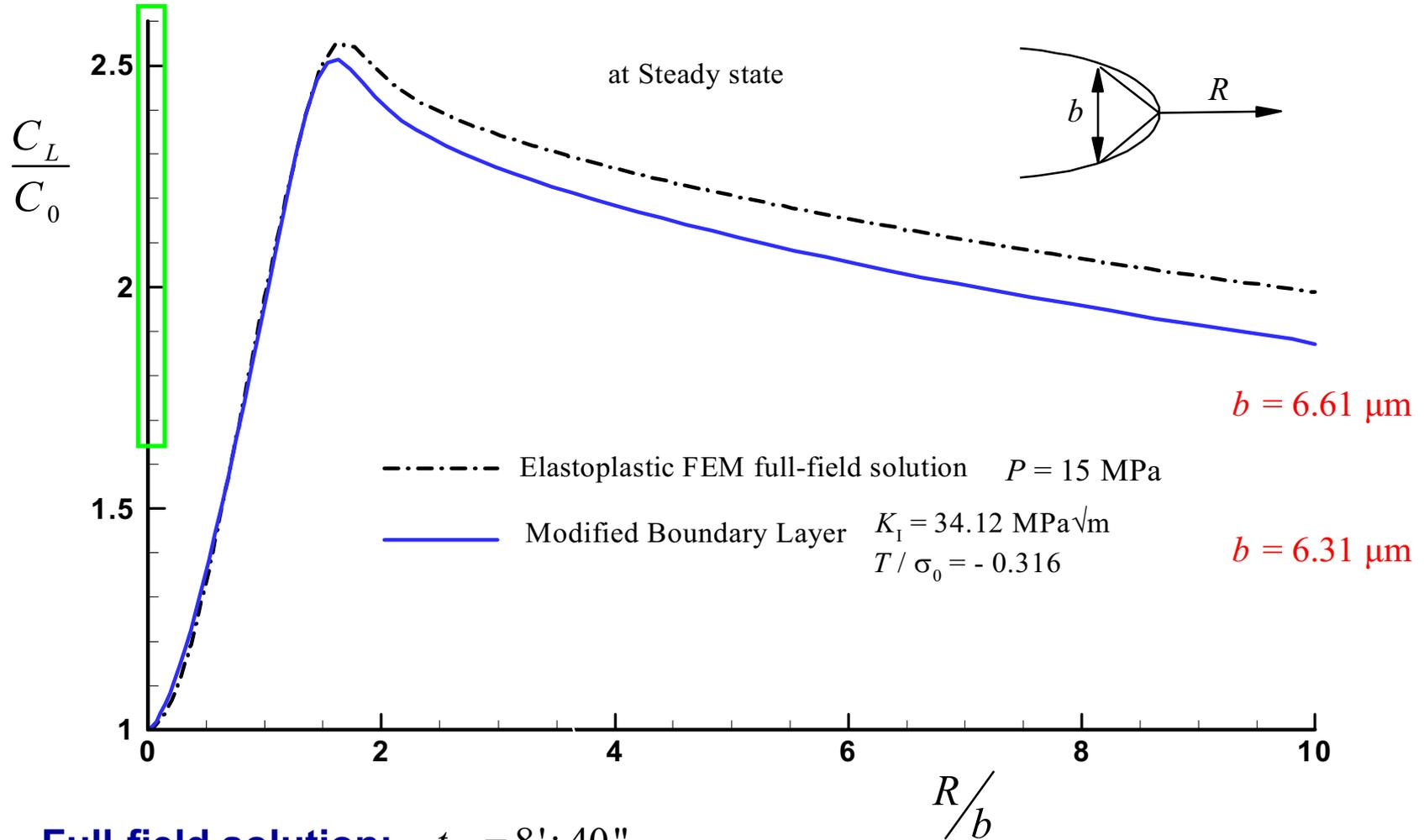


Full Field (pipeline) vs Boundary Layer Solution (laboratory specimen)

Neglecting the T -stress in the MBL formulation fails to predict the true stress



Full Field (pipeline) vs Boundary Layer Solution (laboratory specimen)



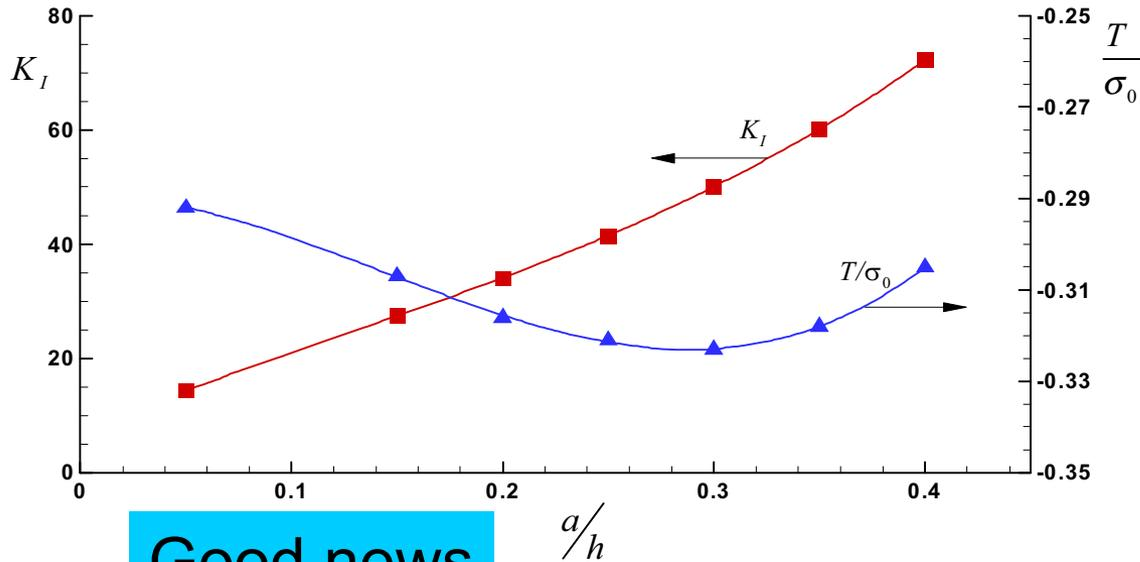
Full-field solution: $t_{ss} = 8':40''$

$a/h = 0.2$

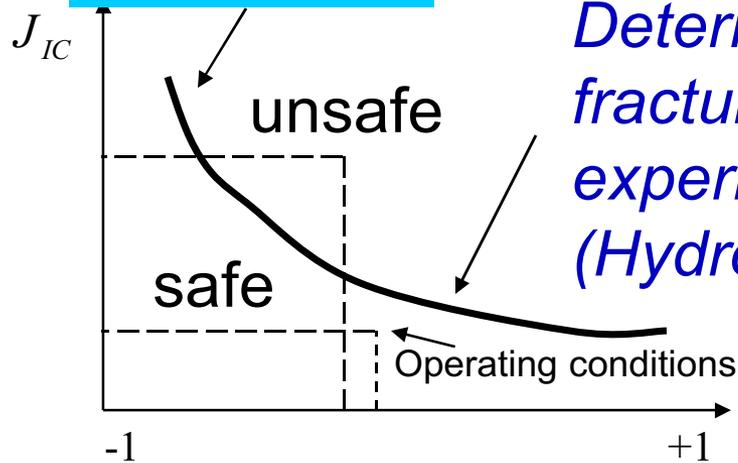
MBL approach: $t_{ss} = 6':40''$

Fracture Mechanics Assessment

Constraint based fracture mechanics: J-T controlled fracture



Good news

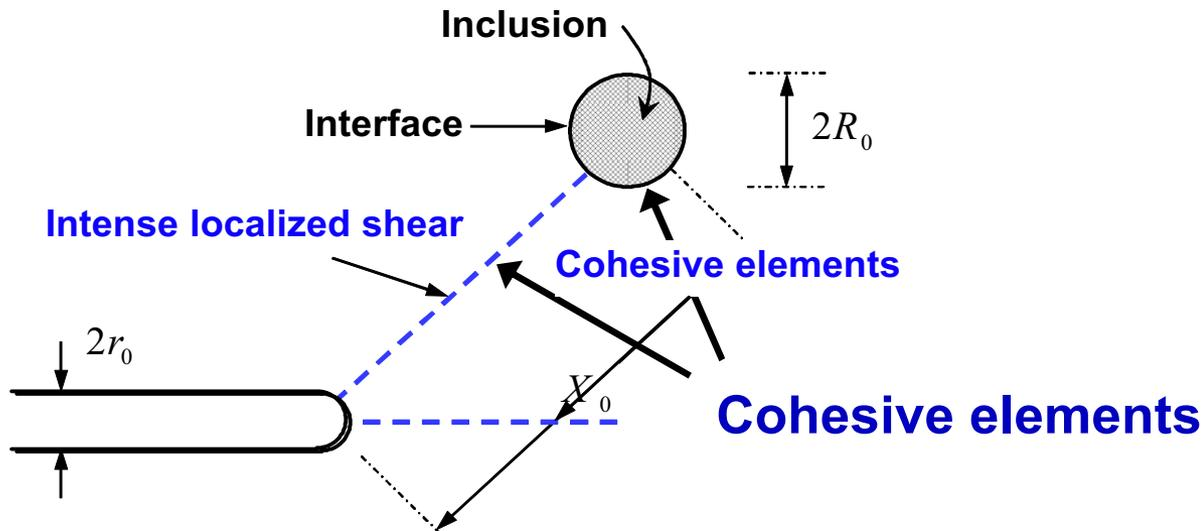


Determine this fracture locus experimentally (Hydrogen effect?)

Laboratory Specimens

- The deep-notch toughness data in the presence of hydrogen need not necessarily lead to a conservative fracture toughness assessment for shallow cracked geometries as is commonly assumed in the absence of hydrogen
- Shallow cracks are attracting hydrogen by plasticity so they, too, are degraded
- Deep-notch cracks are attracting hydrogen by the hydrostatic constraint

Modeling the Fracture Process



$$T_n = \frac{\sigma(c, q) u_n}{q \delta_n}$$

$$T_t = \frac{\delta_n \sigma(c, q) u_n}{\delta_t q \delta_t}$$

$$q = \sqrt{\left(\frac{u_n}{\delta_n}\right)^2 + \left(\frac{u_t}{\delta_t}\right)^2}$$

Transient separation

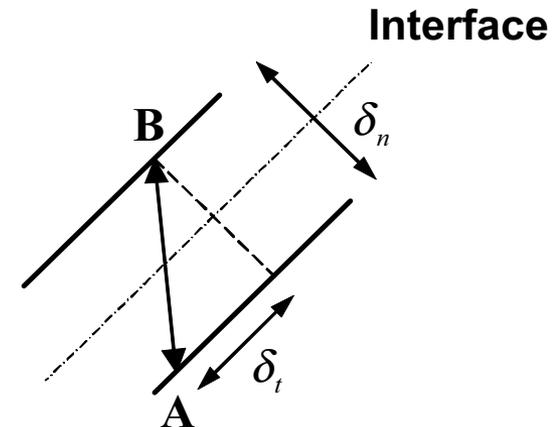
[Mishin *et al.*, 2002]

$$\sigma(c, q) = \frac{27}{4} \sigma_{\max} [1 + (\kappa - 1)c] q (1 - q)^2$$

σ_{\max} : Maximum cohesive stress

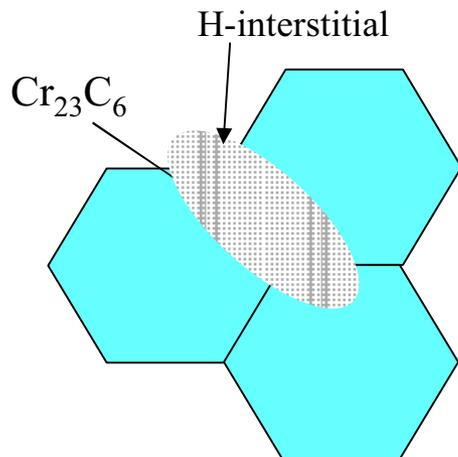
$$\kappa = \frac{\text{cohesive energy with } c = 1}{\text{cohesive energy with } c = 0}$$

First Principles Calculations



First Principles Calculations

- **Assessment of interfacial strength of second-phase particles in pipeline steels in hydrogen**
 - Ferrite-based alloys have Cr_{23}C_6 and MnS precipitates at grain boundary interfaces. Substitutional solutes (e.g. Cr, Mn, Si) or interstitials (e.g. H, N, C) modify structure and stability
 - H (N or C) interstitials alter bonding and cohesion
 - Cr is depleted near Cr_{23}C_6 interface while Fe preferentially occupies Cr sites not bonded to C
 - Obtain cohesive energies via first-principles, Density Functional Theory (DFT) calculations with distribution of atoms near interfaces based on periodic cell approximations
- **Calibration of phenomenological parameters in the thermodynamic theory of decohesion of Mishin et al. (200)**
- **Validation of ab-initio calculations for decohesion energy calculations**
 - Unrelaxed binding energies (eV) and their differences for H in Fe grain boundary (GB) and free surface (FS) calculated by VASP PAW-GGA and FLAPW (Zhong *et al.*, 2000).



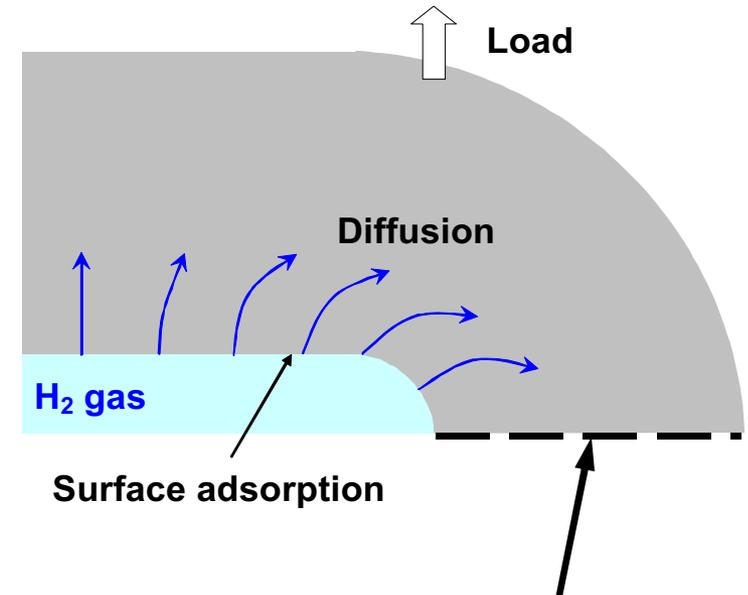
		GB	FS	GB-FS
Unrelaxed binding energies	VASP PAW-GGA	-3.23	-3.57	+0.34
	FLAPW GGA (Zhong <i>et al.</i> , 2000)	-3.09	-3.42	+0.33

Time Scales

t_a : characteristic time of adsorption

t_L : loading rate

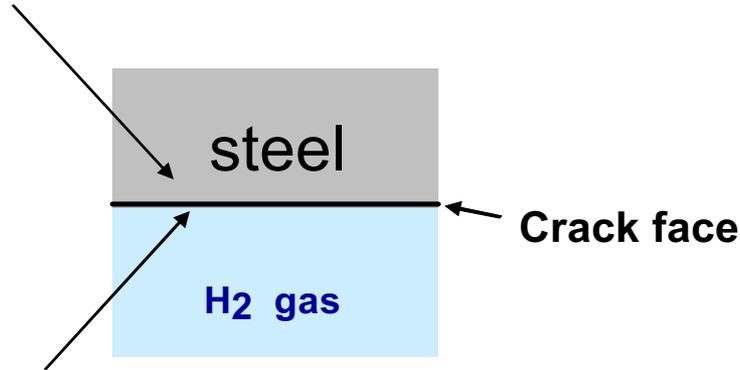
t_D : characteristic diffusion time $\propto \frac{1}{D_{eff}}$



Effect of time scales on mechanics of crack initiation and growth

Hydrogen Adsorption

$$\mu = \mu_0(\Theta) + R\Theta \ln(c_L) - \sigma_{kk} V_H / 3$$



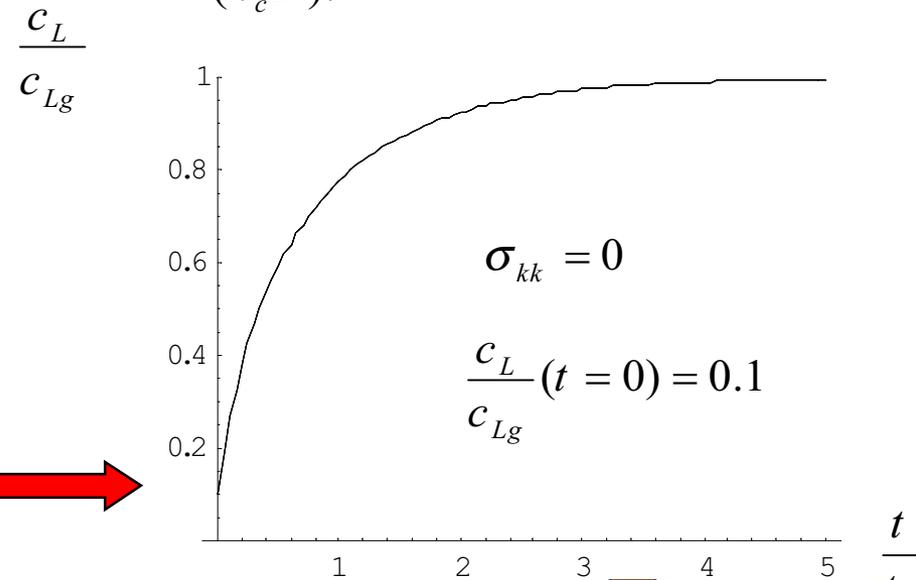
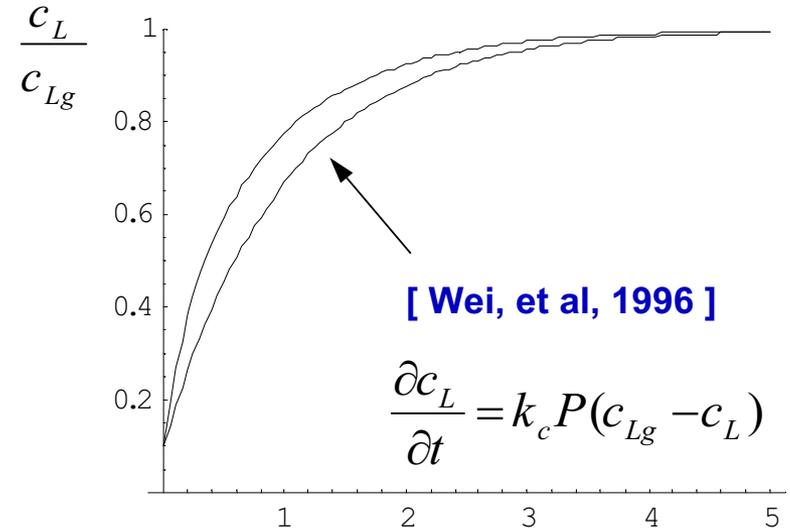
$$\mu_g = \mu_0(\Theta) + R\Theta \ln(c_{Lg})$$

$$c_{Lg} \propto \sqrt{f}$$

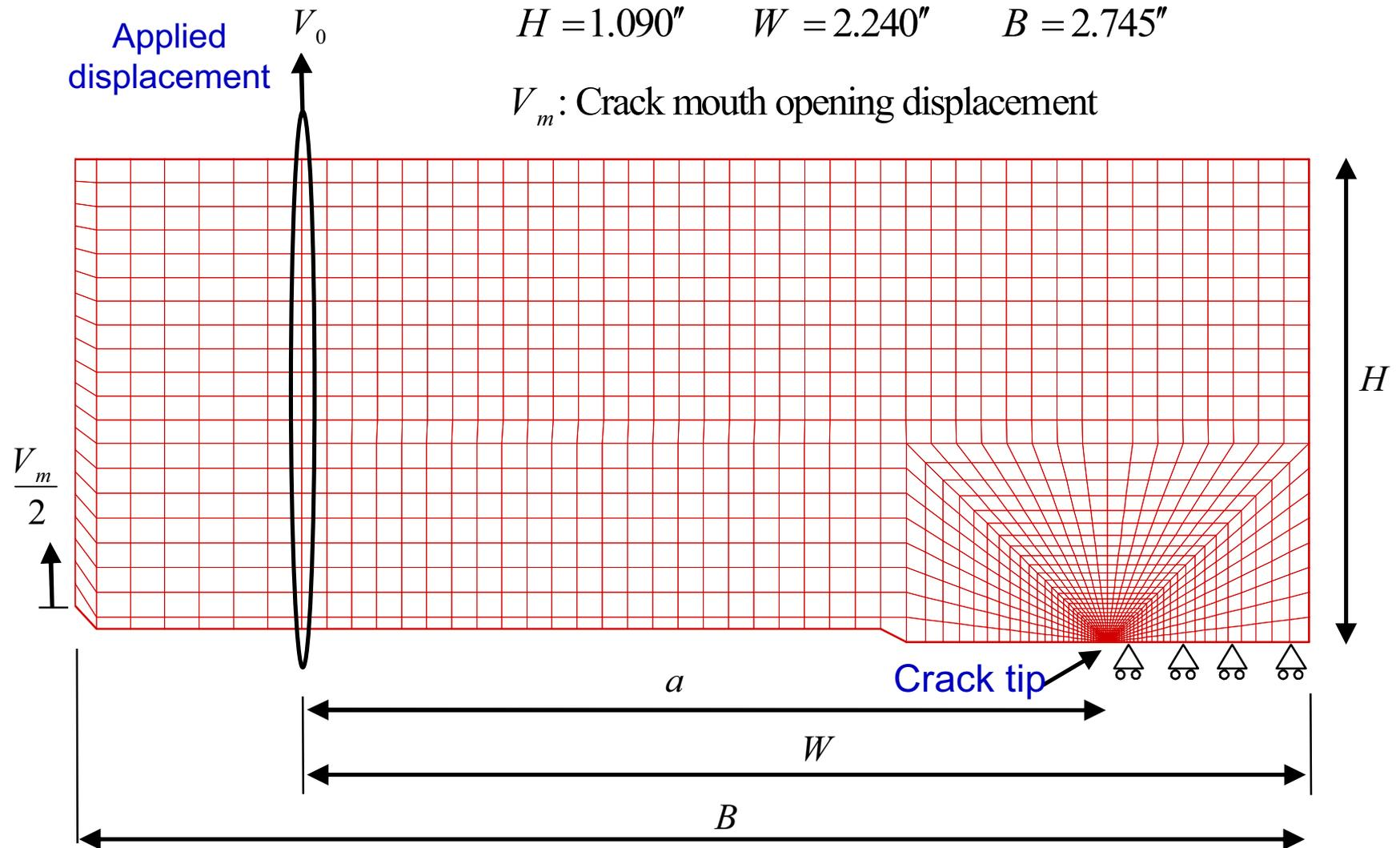
$$\frac{\partial c_L}{\partial t} = \frac{1}{t_a R \Theta} (\mu_g - \mu)$$

t_a : characteristic adsorption time

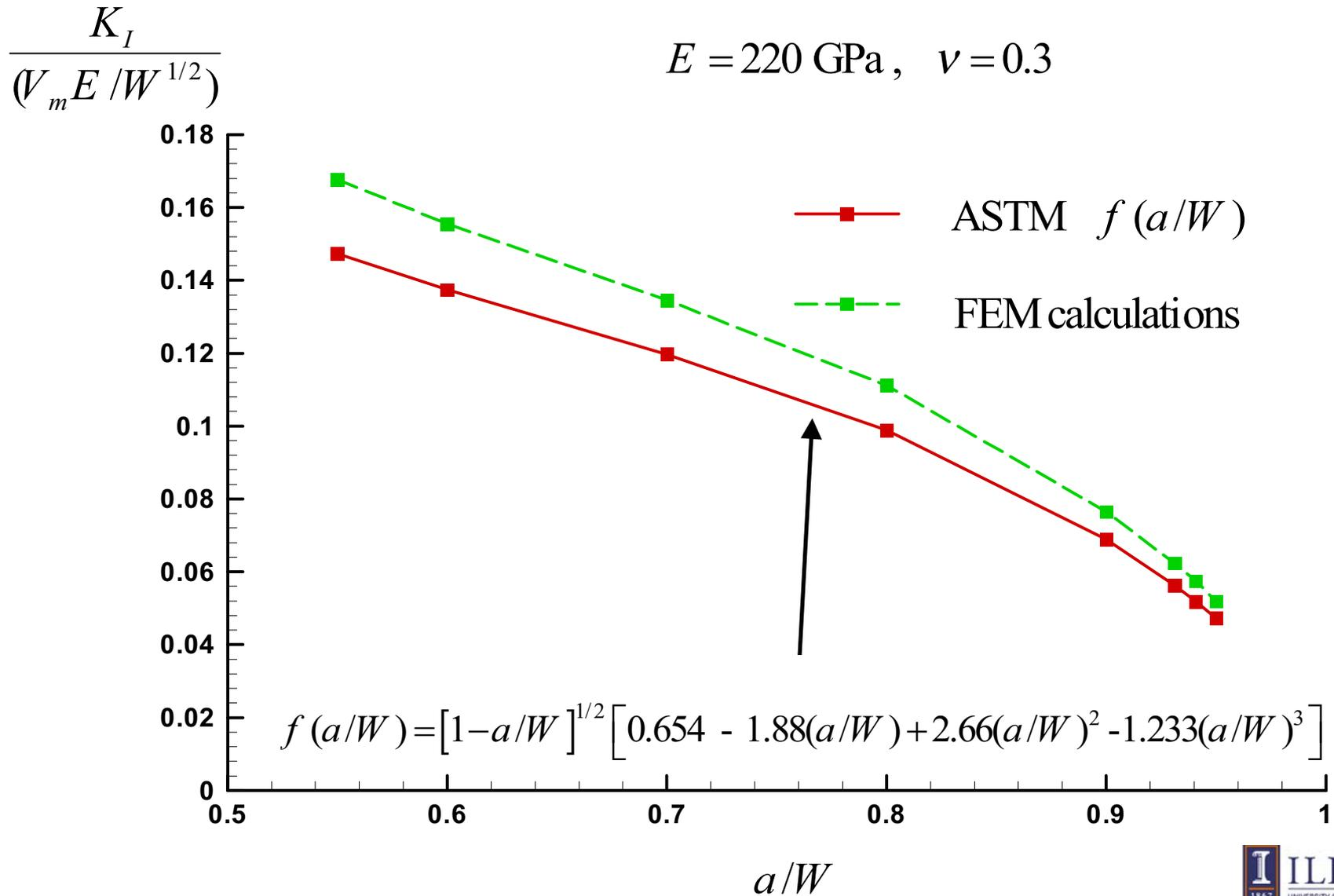
$$\frac{\partial c_L}{\partial t} = \frac{1}{t_a} \left[\ln(c_{Lg} / c_L) + \sigma_{kk} V_H / 3R\Theta \right]$$



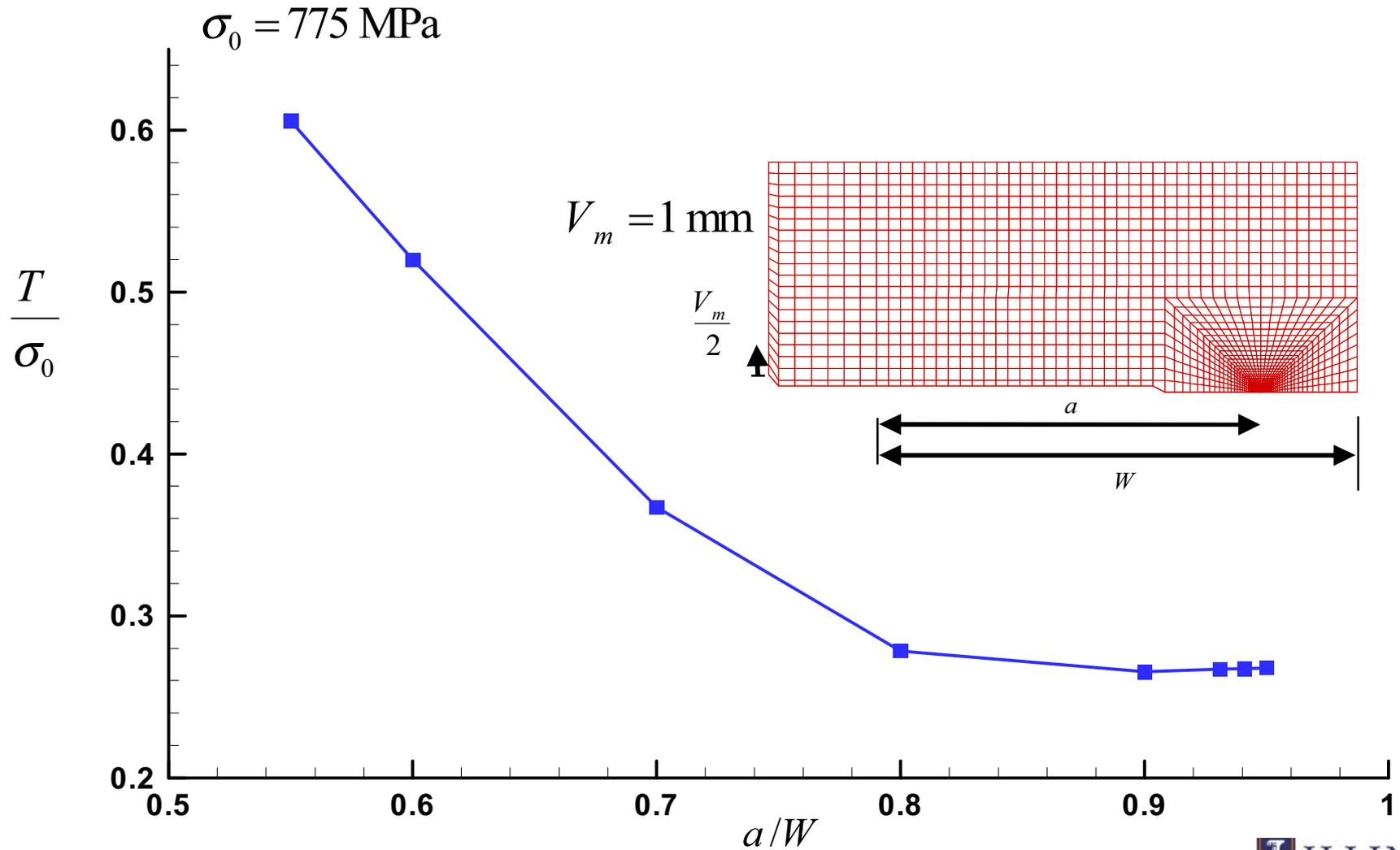
WOL Specimen for Subcritical Crack Growth Finite Element Mesh



Comparing FEM Result with ASTM Equation



Normalized T-stress for specific V_m – FEM Calculations



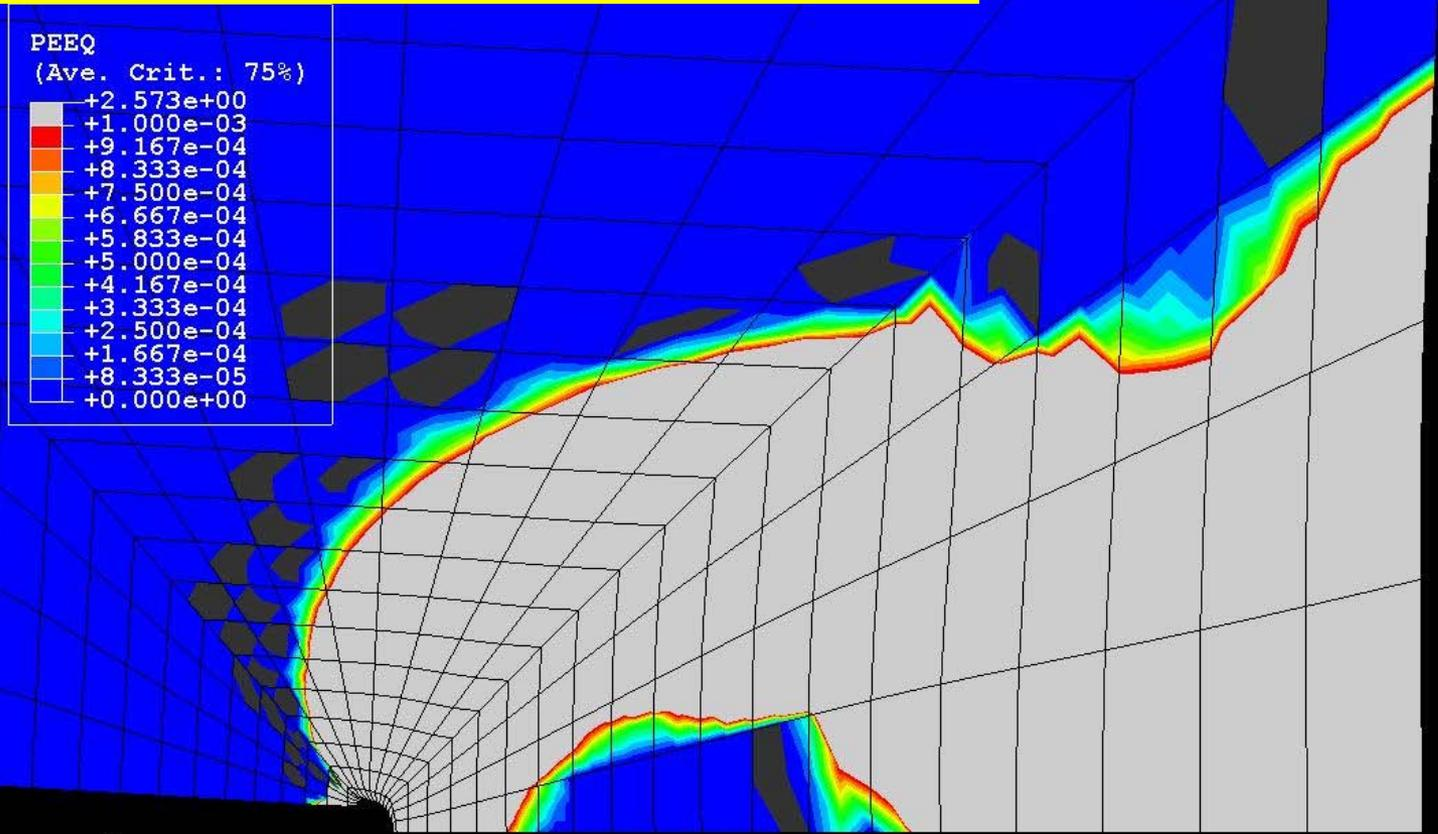
FEM Results for increased load of SNL Exp-2

$$V_m = 4.9582\text{mm} \quad a/W = 0.9408$$

$$\xrightarrow{\text{ASTM}} K_I = 236.9 \text{ MPa}\sqrt{\text{m}}$$

$$\xrightarrow{\text{FEM}} K_I = 261.8 \text{ MPa}\sqrt{\text{m}}$$

Loss of both K - and J -dominance



FEM (Plastic)

$$J = 124000 \text{ N/m}$$

$$K_I = \sqrt{\frac{JE}{1-\nu^2}}$$

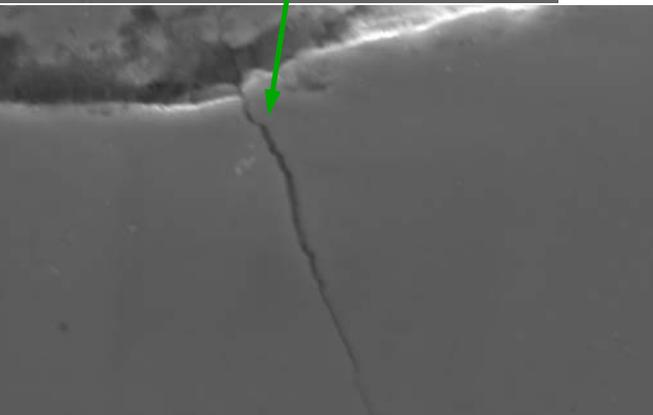
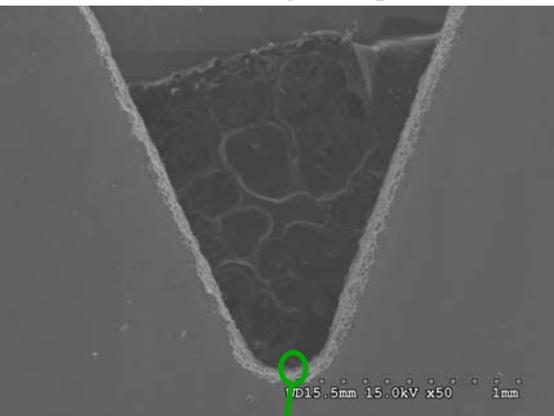
$$K_I = 170 \text{ MPa}\sqrt{\text{m}}$$

Conclusions and Future Work

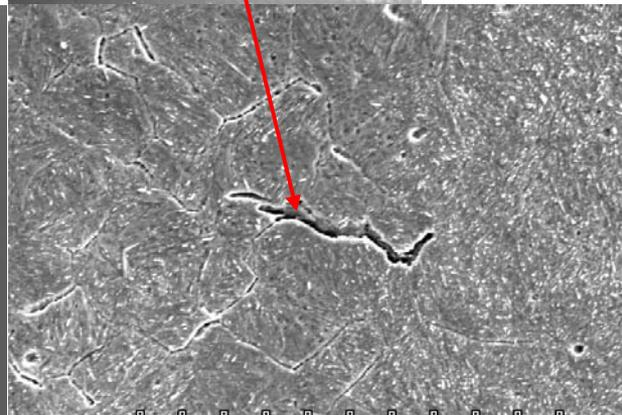
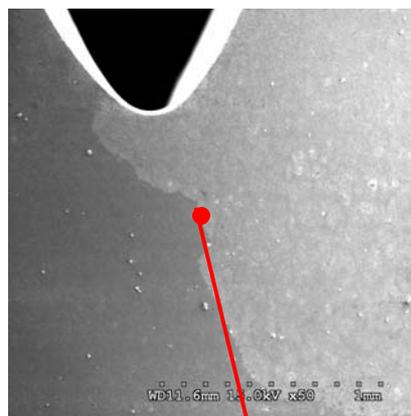
- **Hydrogen adsorption and transport methodology**
 - Interaction of time scales
 - Possible effects on remediation
- **Mechanisms of fracture (microstructural characterization)**
 - Material system dependence
 - Steel microstructure
 - Weldment
 - Load mode dependence (static vs fatigue)
 - Mode of hydrogen uptake (subcritical crack growth)
- **Coupling mechanisms with transport to understand**
 - Crack initiation
 - Crack propagation
 - Devise fracture criteria with predicting capabilities
 - Possibly a $J_{IC}-T$ locus
- **Fracture mechanics/mechanism-based approach to design**
 - As opposed to the SMYS approach

Hydrogen-Induced Degardation in 4340 Steel

- Studies on the mechanical properties of high-strength steel (AISI 4340) characterize the marked deterioration in fracture strength with increase in hydrogen concentration.
- Mechanical properties are used in the statistical model of hydrogen-assisted fracture

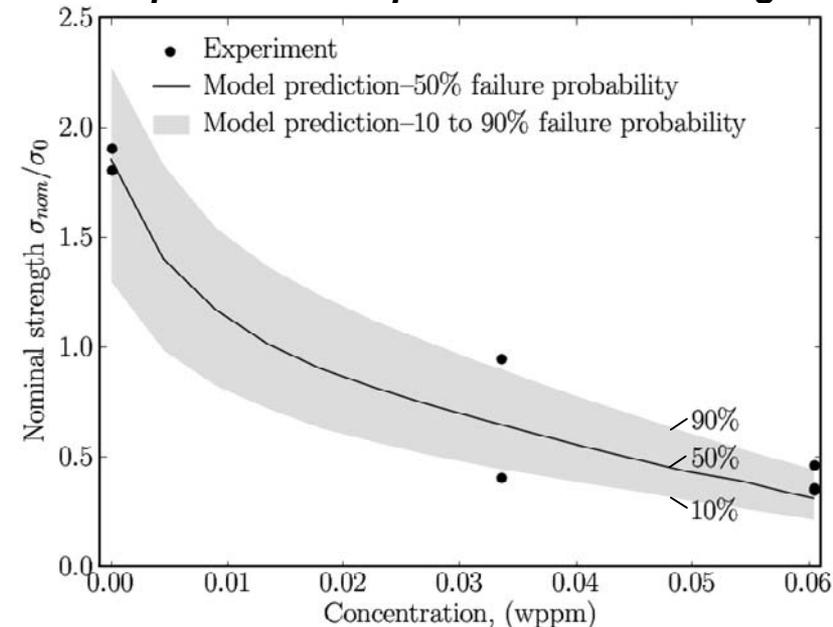


Hydrogen free

5 μm 

Hydrogen charged

Results for 4-point Bend Single Notched Specimens: Experiment vs Modeling



Mechanistic Aspects

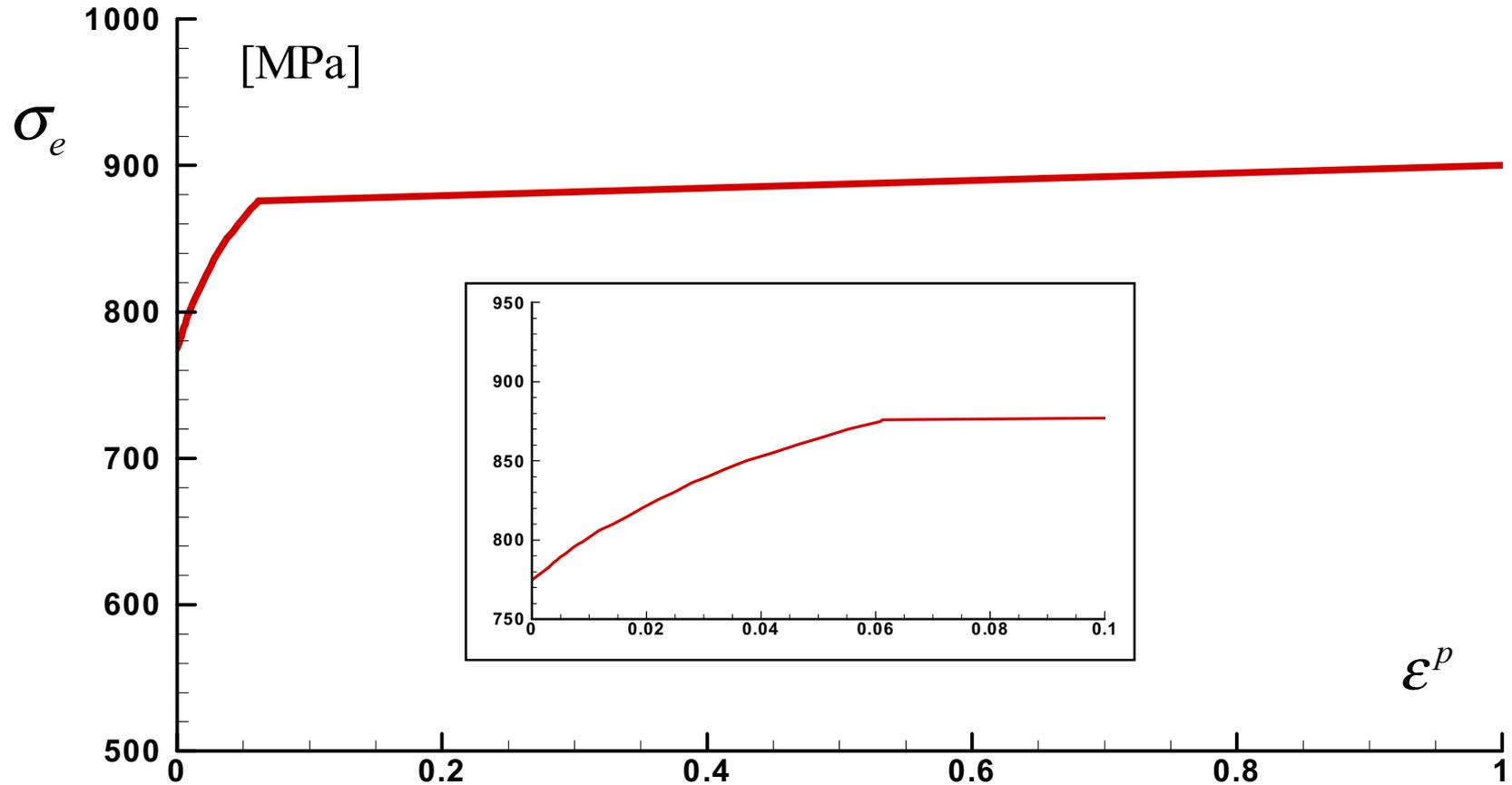
- double-notch bend testing shows that without H, fracture is *strain-controlled*, *i.e.*, initiation occurs at the notch (left)
- with H, fracture is inter-granular and *stress-controlled*; initiation occurs ahead of the notch (right)

Additional slides

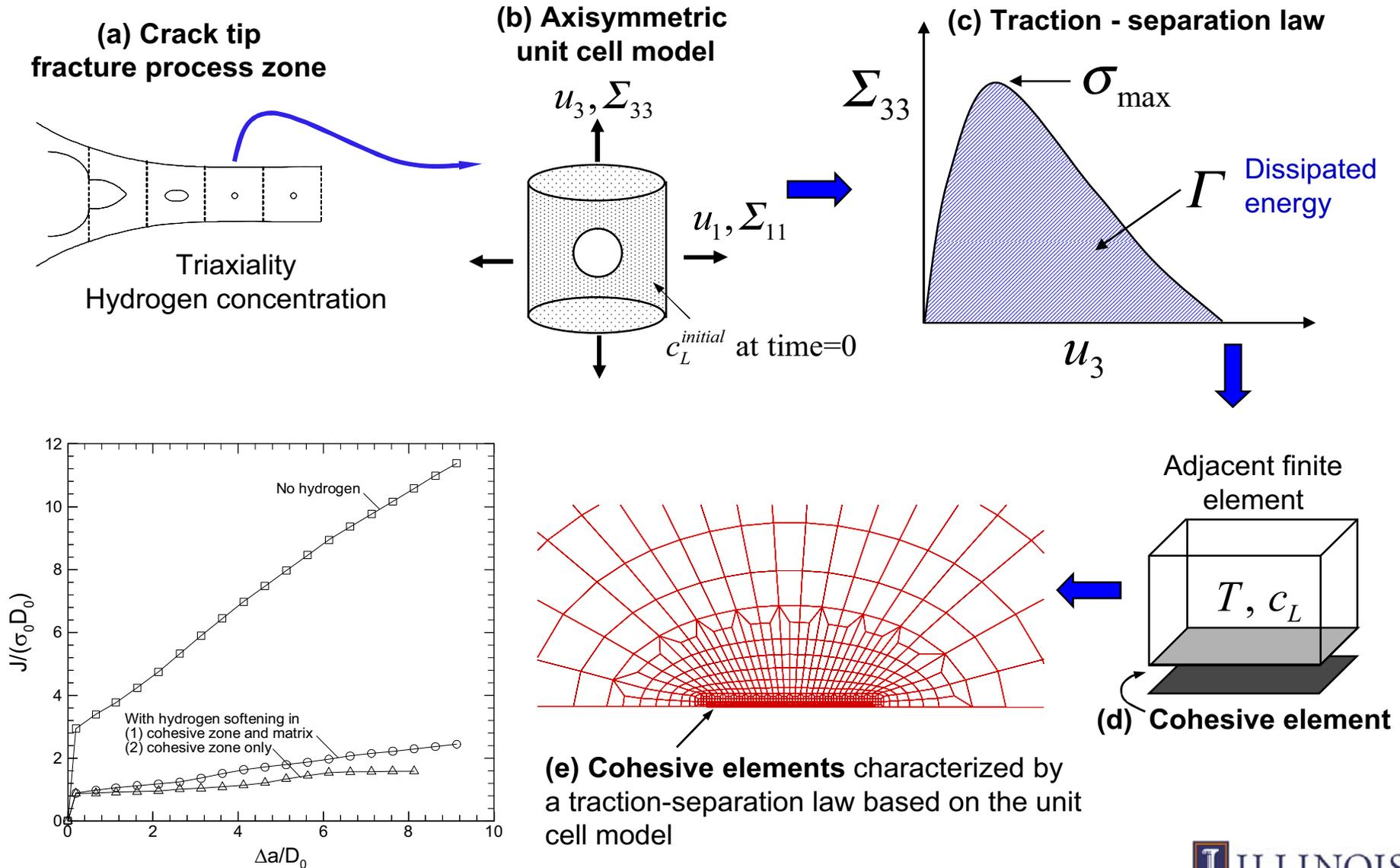
Conclusions on WOL

- **Abaqus result on K seems to be correct**
 - See comparison with the compact tension specimen which we “assume” has a more accurate calibration function
- **We do have K dominance even for a crack of $a/w=0.94$**
 - This is not the case for X-52 at such large a/w
- **An important outcome is that we have both K and T. In combination with the experiment we can explore criticality conditions based on two parameter characterization**
 - Study the hydrogen effect on this two-parameter characterization

Stress – plastic strain curve



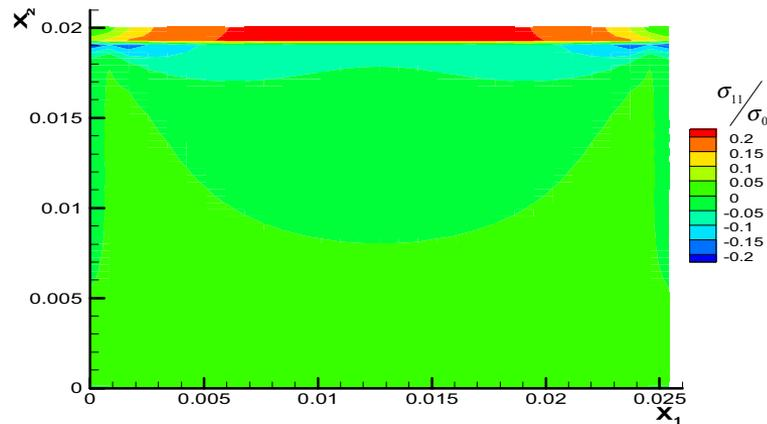
Long Term Objective: Multiscale Fracture Approach



Future Work

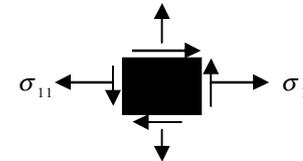
Other Activities

- Finite element analysis of residual stresses of a Schott Coating sitting on the substrate



Average tensile stress σ_{11} in the coating is 125 MPa

Note that substrate is under large compression (-100MPa) at the edges (possible delamination cause)



- Continue collaboration with ASME on establishing guidelines for codes and standards

Continue our ongoing collaboration with the Japan program for materials solutions for the Hydrogen Economy

- Hydrogen National Institute for Use and Storage (**Hydrogenius**)

➤ Kyushu University (Prof. Y. Murakami)

Continue our ongoing collaboration with the NATURALHY Project sponsored by the European Union

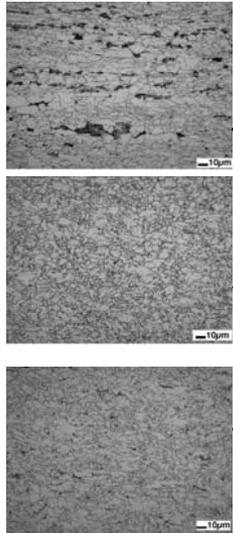
- Interaction of hydrogen in a pipeline with a corrosion induced-crack on the external wall

Future Work

■ Experiment

● Establish the diffusion characteristics of existing and new pipeline steel microstructures

- Existing pipeline steel samples provided by **Air Liquide** and **Air Products**. Specimens are in our laboratory
- New micro-alloyed steels (new microstructures) provided by Oregon Steel Mills through DGS Metallurgical Solutions, Inc.



	API/ Grade	C	Mn	Si	Cu	Ni	V	Nb	Cr	Ti
A	X70	0.08	1.53	0.28	0.01	0.00	0.050	0.061	0.01	0.014
B	X70/80	0.05	1.52	0.12	0.23	0.14	0.001	0.092	0.25	0.012
C	X70/80	0.04	1.61	0.14	0.22	0.12	0.000	0.096	0.42	0.015
D	X52/60	0.03	1.14	0.18	0.24	0.14	0.001	0.084	0.16	0.014

Typical natural gas pipeline steel
 Ferrite/acicular ferrite
 Ferrite/acicular ferrite
 Ferrite/low level of pearlite

- **Collaboration with ORNL and Schott North America for coating of our samples**

- **Determine uniaxial tension macroscopic flow characteristics in the presence of hydrogen**
- **Carry out fracture testing: Collaboration with Sandia, Livermore**
- **SEM and TEM studies on existing and new pipeline material microstructures**
 - Fracture surfaces, particle, dislocation, and grain boundary characterization

Additional slides

Critical Assumptions and Issues

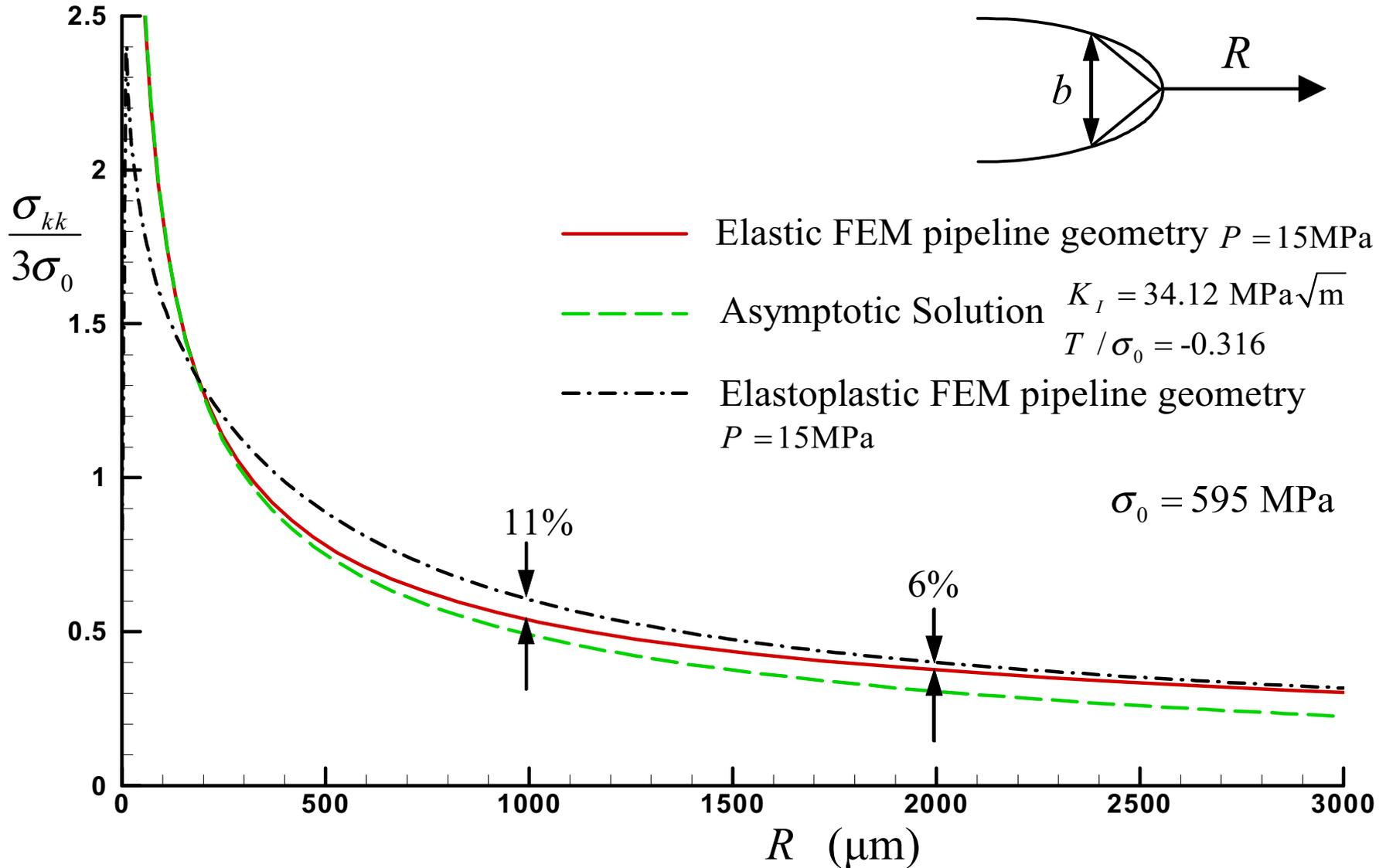
- **Hydrogen-induced cracking in existing pipeline steels initiates at second phase particles by hydrogen-induced decohesion followed by shear localization of ligaments**
 - **Fracture toughness testing and SEM/TEM studies will verify this assumption**

- **Embrittlement of acicular ferrite initiates at the needle-pearlite/ferrite interface**
 - **Fracture toughness testing and SEM/TEM studies will verify this assumption**

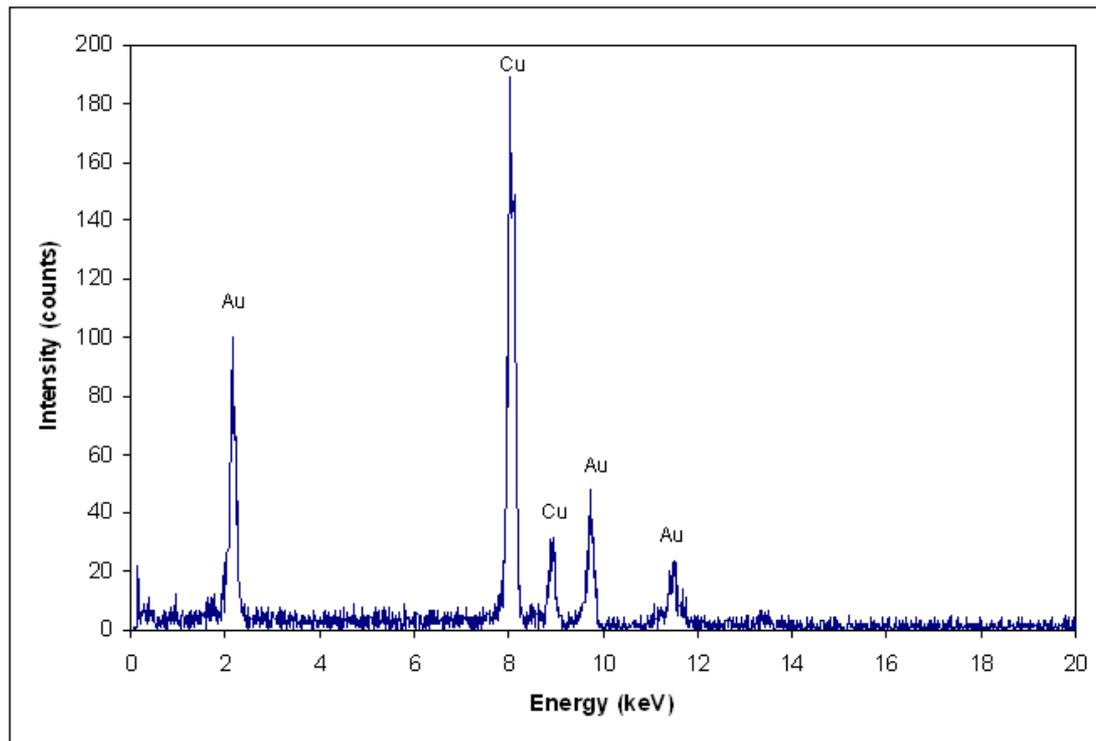
- **Hydrogen dramatically degrades the resistance of steel to fatigue crack growth. Possible remediation by water vapor and oxidation**
 - **Experiments to study the oxidation effects**

- **Lack of funding does not allow**
 - **Hire personnel**
 - **Construct experimental devices**
 - **Carry out testing**

Ahead of the crack tip

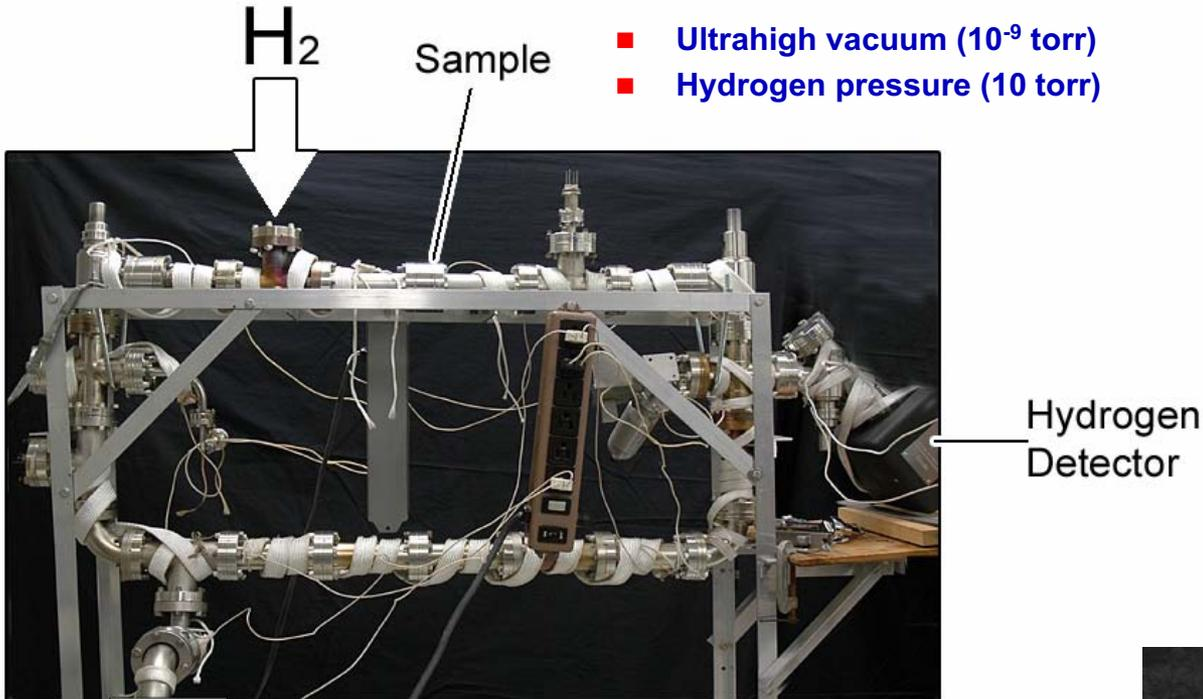


EDS reference



EDS of gold sample showing copper peaks from sample holder

Permeation

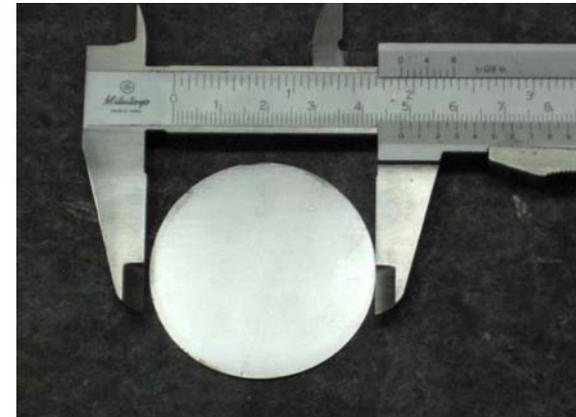


- Ultrahigh vacuum (10^{-9} torr)
- Hydrogen pressure (10 torr)

- Hydrogen is introduced on one side of the sample
- Permeates through sample
- Detected by ion pump

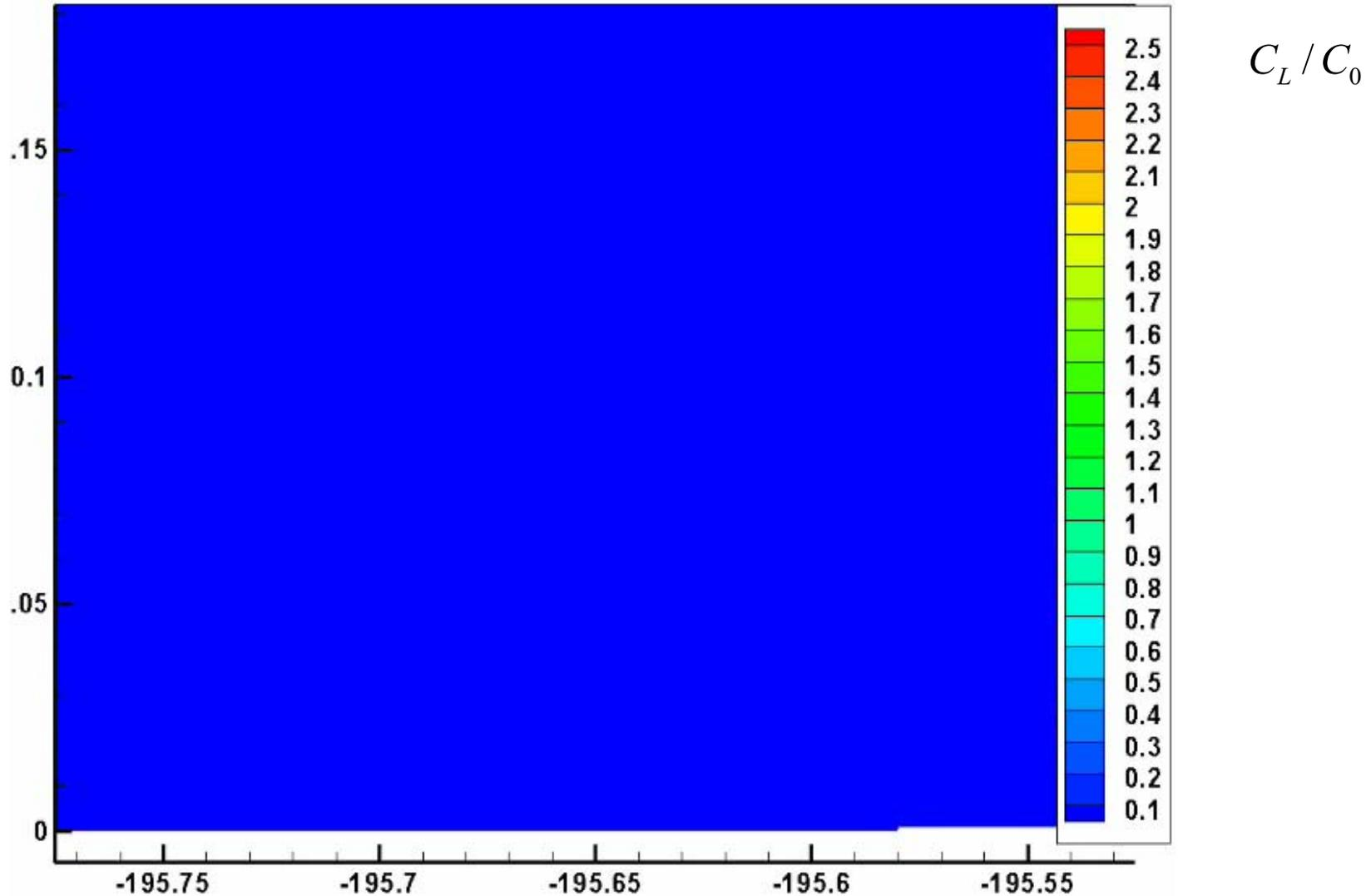
Turbo
pump

- 4.75 cm disks
- 100 micron thickness
- Palladium coating on exit side
- Testing coatings on hydrogen side

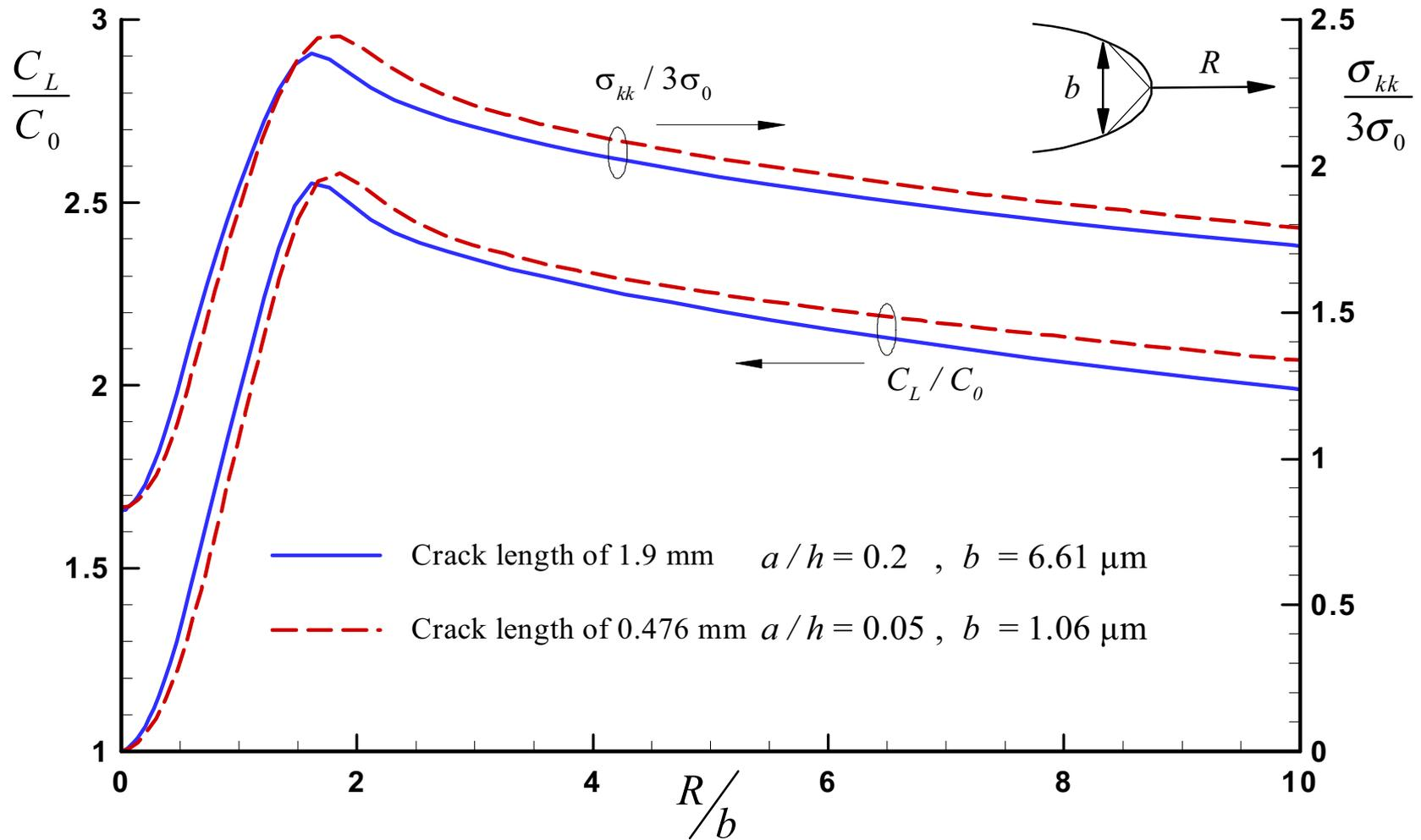


Real-world pipeline specimens are in our possession for testing
Air Liquide and **Air Products** provided the coupons

Transient to Steady State - Lattice Concentration



Full Field (pipeline) vs Boundary Layer Solution (laboratory specimen)



$a/h = 0.2$

$$K_I = 34.12 \text{ MPa}\sqrt{\text{m}}$$

$$T/\sigma_0 = -0.316$$

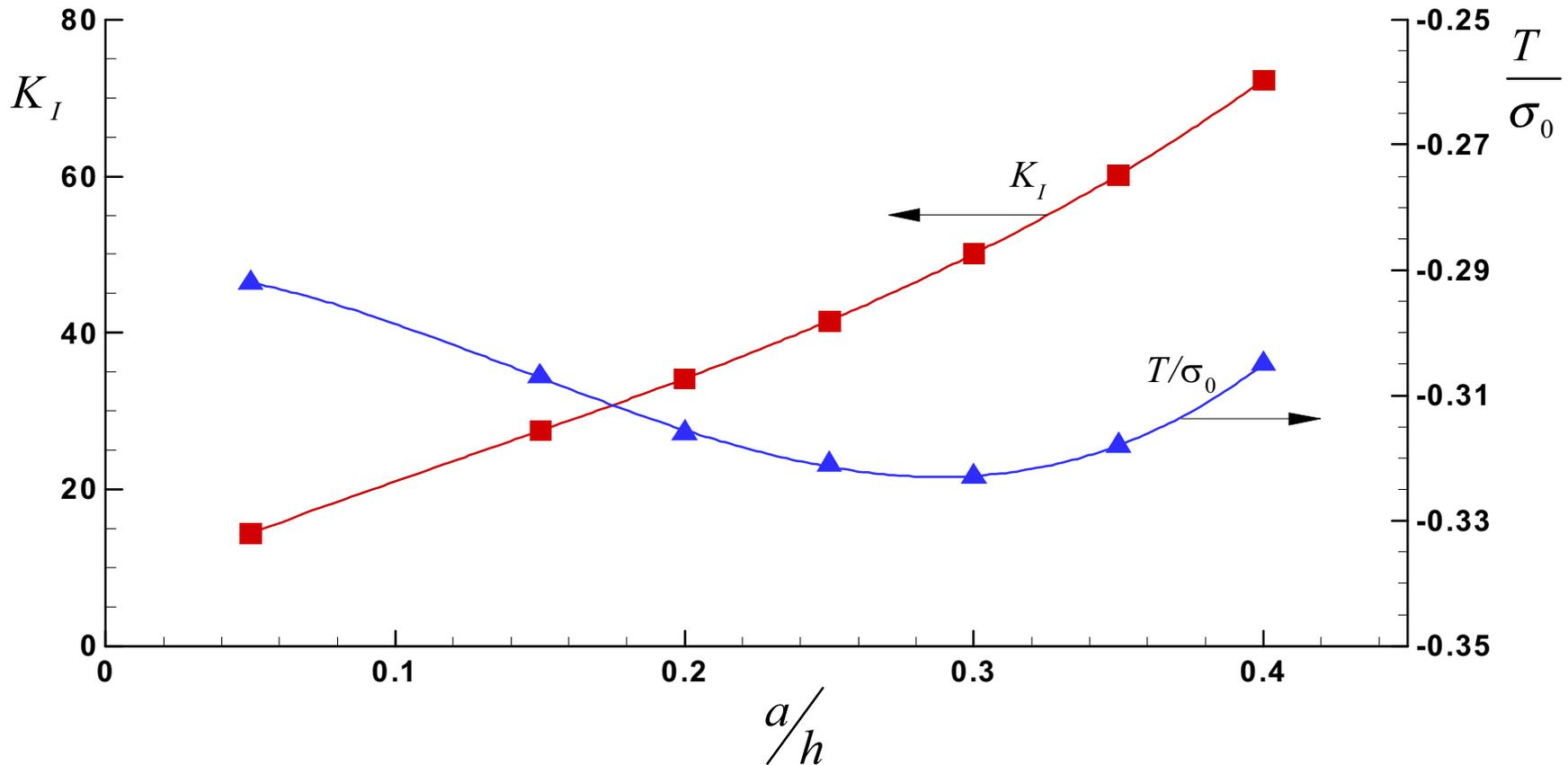
$a/h = 0.05$

$$K_I = 14.38 \text{ MPa}\sqrt{\text{m}}$$

$$T/\sigma_0 = -0.292$$

Fracture Assessment

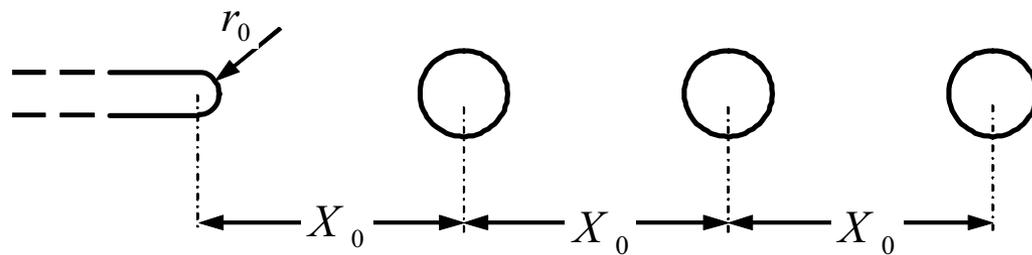
From the full pipeline to laboratory specimens



Crack depth/pipeline thickness

Hydrogen effect on ductile crack growth

- crack growth mechanisms
 - Void by void growth
 - Multiple void growth



void population

A diagram showing three circular voids. The first void on the left has a vertical double-headed arrow indicating its diameter as $2R_0$. Below the diagram, the void population fraction is given by the equation:

$$f_0 = \pi(R_0 / X_0)^2$$

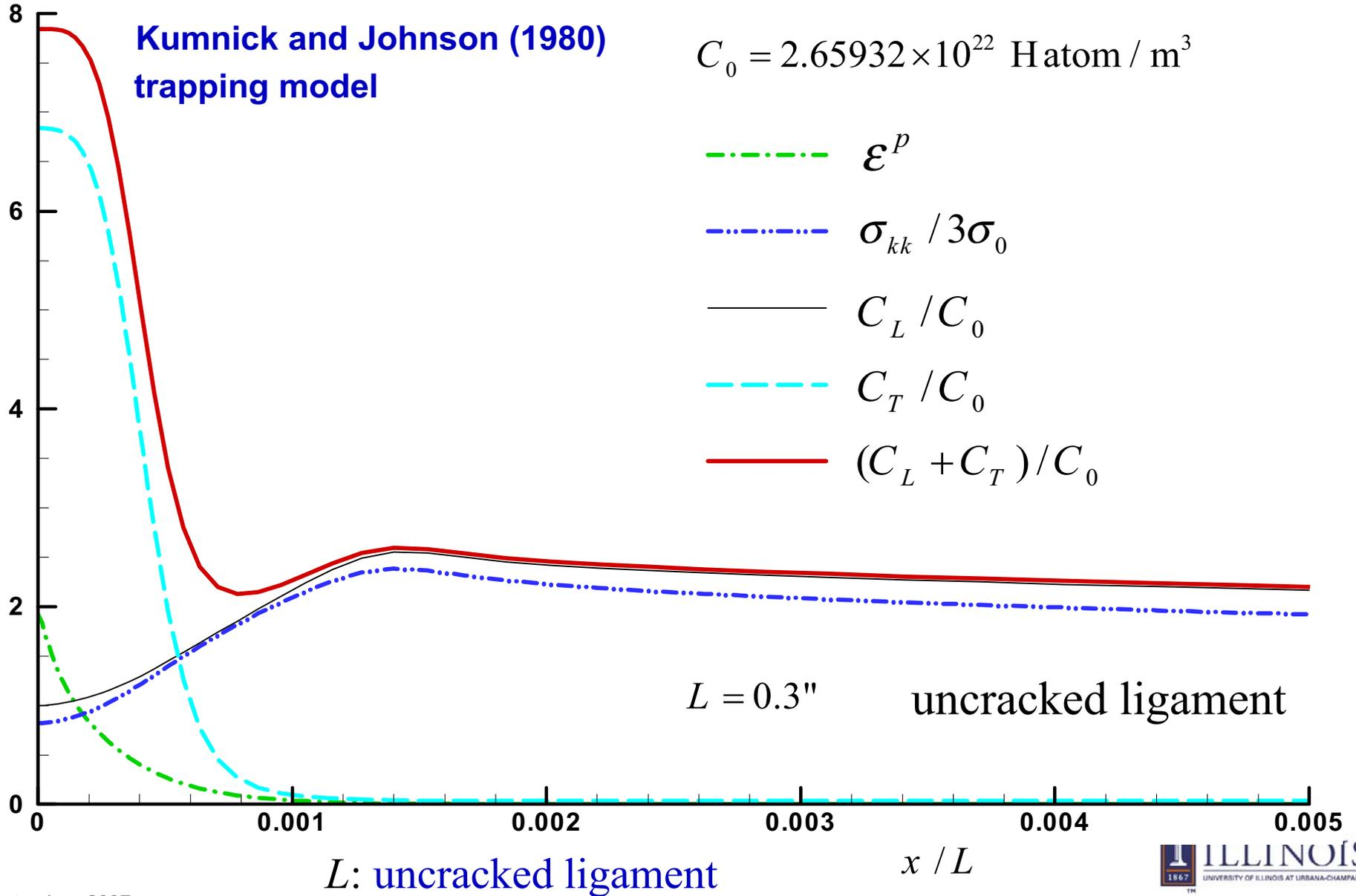
[Tvergaard and Hutchinson, 2002
Petti and Dodds, 2005]

- Effect of hydrogen softening and dilatation
- Identifying the range of f_0 that each mechanisms is operative

Ab-initio

- We have completed several necessary validation “computer experiments” on the binding energies for H in Fe grain boundary and free surface using a pseudopotential based plane-wave method via projected-augmented wave basis functions, as implemented in the Vienna *ab initio* Simulation Package. A subset of our validation results provides unrelaxed binding energies for H in Fe for GB/FS equal to -3.23/-3.57 eV, and the binding energies difference of the GB and FS equal to +0.34 eV, in good agreement with values in literature [4].

Ahead of the crack tip at steady state



Compact Tension Specimen: FEM Result vs Handbook

